INSTITUTO NACIONAL DE PESQUISAS DA AMAZÔNIA

PROGRAMA DE PÓS-GRADUAÇÃO EM ECOLOGIA

Integração funcional da arquitetura hidráulica em árvores de platô e baixio na Amazônia Central

MATHEUS GUTHIERRIS BITENCOURT ROSA

MANAUS, AM

NOVEMBRO, 2023

MATHEUS GUTHIERRIS BITENCOURT ROSA

Integração funcional da arquitetura hidráulica em árvores de platô e baixio na Amazônia Central

Orientadora: Dra. Juliana Schietti de Almeida

Dissertação apresentada ao Instituto Nacional de Pesquisas da Amazônia como parte dos requisitos para obtenção do título de mestre em Biologia (Ecologia).

MANAUS, AM

NOVEMBRO, 2023

PROGRAMA DE PÓS-GRADUAÇÃO EM ECOLOGIA

ATA DA DEFESA PÚBLICA DA DISSERTAÇÃO DE MESTRADO DO PROGRAMA DE PÓS-GRADUAÇÃO EM ECOLOGIA DO INSTITUTO NACIONAL DE PESQUISAS DA AMAZÔNIA.

Aos 21 dias do mês de novembro do ano de 2023, às 09:h00min, via videoconferência, reuniu-se a Comissão Examinadora de Defesa Pública, composta pelos seguintes membros: a **Drª. Flávia Regina Capellotto Costa**, do Instituto Nacional de Pesquisas da Amazônia – INPA, a **Drª. Thaise Emilio Lopes de Sousa**, da Universidade Federal do Rio de Janeiro – UFRJ e o **Dr. Christopher Baraloto**, da Universidade Internacional da Flórida – FIU, tendo como suplentes a Drª. Gisele Biem Mori (INPA) e o Dr. Adriano Costa Quaresma (INPA), sob a presidência da orientadora, a fim de proceder a arguição pública do trabalho de **DISSERTAÇÃO DE MESTRADO** de **MATHEUS GUTHIERRIS BITENCOURT ROSA**, intitulado: **"INTEGRAÇÃO FUNCIONAL DA ARQUITETURA HIDRÁULICA EM ÁRVORES DE PLATÔ E BAIXIO NA AMAZÔNIA CENTRAL"**, orientado pela Drª. Juliana Schietti de Almeida, da Universidade Federal do Amazonas – UFAM.

Após a exposição, o(a) discente foi arguido oralmente pelos membros da Comissão Examinadora, tendo recebido o conceito final:

[X] APROVADO (A) [ ] REPROVADO (A)

[X] POR UNANIMIDADE [ ] POR MAIORIA

Nada mais havendo, a presente ata foi lida, lavrada e assinada pelos membros da Comissão Examinadora.

DRª. FLÁVIA REGINA CAPELLOTTO COSTA _____

DRª. THAISE EMILIO LOPES DE SOUSA _____

DR. CHRISTOPHER BARALOTO _____

DRª. GISELE BIEM MORI _____

DR. ADRIANO COSTA QUARESMA _____

_____
(Coordenação PPG-ECO/INPA)

Catalogação na Publicação (CIP-Brasil)

R788i Rosa, Matheus G B
Integração funcional da arquitetura hidráulica em árvores de platô e baixio na Amazônia Central / Matheus Guthierris Bitencourt Rosa; orientadora Juliana Schietti de Almeida. - Manaus: [s.l.], 2023.

2.0MB
57p. : il. color.

Dissertação (Mestrado - Programa de Pós-Graduação em Ecologia) - Coordenação do Programa de Pós-Graduação, INPA, 2024.

1. Ecologia funcional. 2. Ecofisiologia vegetal. 3. Arquitetura hidráulica. I. Almeida, Juliana Schietti de. II. Título

CDD 551.48 811 3

Sinopse:

Estudamos o padrão de integração entre múltiplas características funcionais associadas ao uso da água em árvores de dossel na Reserva Florestal Adolpho Ducke, Manaus, Amazônia Central. Comparamos as diferenças nas redes de integração da arquitetura hidráulica de espécies associadas a habitats hidrologicamente contrastantes (platôs e baixios).

Palavras-chave: redes de correlação, características funcionais, arquitetura hidráulica, integração funcional, árvores de dossel

“Quando nós falamos tagarelando
E escrevemos mal ortografado
Quando nós cantamos desafinando
E dançamos descompassado
Quando nós pintamos borrando
E desenhamos enviesado
Não é por que estamos errando
É porque não fomos colonizados.”
– Mestre Nego Bispo

AGRADECIMENTOS

Laroyê, que esse caminho permaneça repleto de encruzilhadas!

Agradeço à minha família, ao meu pai e mãe José Rocha e Malvina Rocha que nutriram um lar saudável na minha infância. Às minhas mães Lucineia e Renata que sempre tiveram presente e incentivando meus estudos desde pequeno. Saúdo as minhas vovós Lázara Bitencourt e Lázara Rosa. E desejo sucesso aos meus irmãos Dudu e Torugo. Agradeço aos meus amigos da graduação que me acolheram em São Paulo quando saí de casa para estudar na capital: Lascada, Caine, Kalau, Poma, Cis, Trans, Stanley, Gina, Mimosa, Camô. Com muito amor do Megas!! Agradeço à minha rede de apoio do CRUSP que fortalecia uns aos outros apesar dos desafios diários do racismo e capitalismo: Araci, Maryellen, Gabizuda, Julia, Aline, Ferícia, Márcio, Kessis, Ristefan. Aos meus amigos da turma de mestrado, pelas conversas sobre nossos projetos, pelos rolês manauaras, Débora, Brenda, Andreza, Liara, Júlia, Amanda, Juçara. Aos meus amigos e companheiros de laboratório, Natália, profa. Flávia, Marcelle, Gabi, Erick, Felipe, Edher, César, Lucas, Cibelly, Clarice. Aos companheiros dos campos que participei na Ducke, no ATTO, no ABC e na UFAM, Mariazinha, Michelle, Zélão, Jardson, Jardel, Ericka, Sâmia, Pietra, Pilar, Joãozinho, Janilson, Deivison, Sr. Sabá, Jesus, Tiago e Lucas. Ao ForrIO & Gafieira, ao Tiago Pety e Vanessinha, à Empire DanceSchool, por tornarem a dança uma parte essencial da minha vida que me ajuda a manter mente e corpo saudáveis.

Por fim, agradeço à minha orientadora, Juju Schietti, pelo acompanhamento e projeto que desenvolvemos, aos professores do PPG-Eco, ao financiamento da CAPES e ao INPA. Sou muito grato por toda minha família e amigos, pelas refeições e muitos momentos compartilhados. Em amor à Amazônia e sua biodiversidade!

Porã-eté aguyjevete. Okê!

RESUMO

A disponibilidade de água no solo tem um impacto significativo em várias características da planta, sendo importante estudar as relações hídricas das plantas numa perspectiva integrativa. Aqui, avaliamos se as características funcionais relacionadas ao uso da água estão funcionalmente integradas em uma rede da arquitetura hidráulica e se espécies associadas a condições contrastantes de disponibilidade hídrica no solo apresentam diferentes padrões de integração de sua arquitetura hidráulica. Analisamos as correlações interespecíficas entre 11 características funcionais em 28 espécies de árvores de dossel associadas a baixios e platôs em uma floresta da Amazônia Central. Usando a matriz de correlações, definimos as características funcionais como os nós de uma rede e as correlações significativas entre pares de características como ligações entre os nós, e calculamos a densidade de ligações da rede, a distância média e o agrupamento médio. Encontramos que as espécies mais altas do dossel investiram em vasos e estômatos grandes e pouco numerosos, casca grossa, folhas com baixa área específica foliar e baixas proporções de área de alburno no tronco. Além disso, espécies de platô mostraram um padrão de integração mais forte com alto agrupamento entre altura, espessura da casca e anatomia de vasos e estômatos, enquanto as espécies de baixio mostraram uma rede mais esparsa, sem nenhuma característica específica apresentando maior importância relativa na topologia da rede. Nossos resultados sugerem que as restrições relacionadas à altura acoplam fortemente o uso da água e do carbono em espécies de dossel, especialmente entre as espécies adaptadas a condições mais secas (platôs) do que entre espécies adaptadas a condições mais úmidas (baixios).

PALAVRAS-CHAVE: redes de correlação, características funcionais, arquitetura hidráulica, florestas tropicais, árvores de dossel, integração funcional

ABSTRACT

Soil water availability has a significant impact on various aspects of the plant phenotype, making it crucial to examine plant water relations from an integrated perspective. Here, we examined whether plant traits related to water-use were functionally integrated into a unified hydraulic architecture network, and evaluated whether species associated with contrasting soil-water conditions had different integration patterns of their hydraulic architecture. We analyzed the interspecific correlations among 11 functional traits of 28 canopy species associated with valleys and plateaus in a Central Amazonian forest. Next, we computed traits as nodes in a network and the significant correlations between pairs of traits as links between nodes, and calculated the network's edge density, average distance and average clustering. When pooling valley and plateau species, taller trees had few larger vessels and stomata, thicker bark, low SLA leaves, and low proportions of stem sapwood area of taller trees. Plateau species exhibited a stronger integration pattern, with high clustering among tree height, bark thickness, and vessel and stomatal traits, while valley species displayed a more sparsely connected network with no specific trait or set of traits holding more relative importance in the network topology. Our results suggest that height-related constraints tightly couple together the water and carbon use in canopy species, especially among species adapted to drier conditions (plateaus) than those adapted to wetter conditions (valleys) in a Central Amazonian forest.

Keywords. trait network, hydraulic architecture, tropical rainforest, canopy trees, functional integration

SUMÁRIO

INTRODUÇÃO GERAL

A arquitetura hidráulica de uma planta é definida pela estrutura do sistema de transporte de água das raízes às folhas, cujo efeito nas relações hídricas das plantas com o solo e a atmosfera deve refletir diferentes estratégias de uso da água (TYREE E EWERS 1991, CRUIZIAT et al. 2002). Além da condução da água no xilema, a forma como a planta armazena água nos tecidos e como ela regula a perda de água nos estômatos são também parte essencial das relações hídricas das plantas (BRODRIBB 2009; PRATT & JACOBSEN 2017; DEANS et al. 2020). Dada a interdependência entre o transporte, o armazenamento e a perda d'água na planta, espera-se que o resultado seja uma arquitetura hidráulica integrada.

Ambientes que apresentam uma estação seca acentuada, passam por um período em que se reduz simultaneamente a disponibilidade hídrica do solo e a umidade relativa do ar, aumentando, dessa forma, a diferença de potencial hídrico do contínuo solo-atmosfera (LAMBERS & OLIVEIRA 2020). Tais condições aumentam a tensão no sistema hidráulico das plantas, podendo acarretar na ocorrência de cavitação (mudança súbita do estado da água líquida para vapor d'água) e embolismos (presença de bolhas de ar nos vasos condutores do xilema) (TYREE & SPERRY 1989). Dado que eventos de cavitação e embolismos caracterizam falha hidráulica, que podem ser irreversíveis e levar à morte da árvore (MCDOWELL et al. 2018), diferentes respostas de curto prazo à queda no potencial hídrico podem permitir à planta evitar a ocorrência de falhas hidráulicas. O fechamento estomático, a liberação de água armazenada nos tecidos e a deciduidade são alguns exemplos (BRODRIBB 2009; POORTER et al. 2014). No entanto, secas extremas e prolongadas podem acarretar também na morte por limitação de carbono se a condutância estomática for mantida em taxas muito baixas (MCDOWELL et al. 2018). Nesse sentido, adaptações coordenadas da anatomia da madeira, das folhas e da casca devem ser importantes para assegurar uma arquitetura hidráulica mais resistente a secas muito severas.

Variações na topografia de um terreno podem determinar diferenças na disponibilidade de água no solo (DAWS et al. 2002), afetando também os padrões de diversidade, composição e distribuição de árvores tropicais ao longo de gradientes topográficos na Amazônia (DE CASTILHO et al. 2006; DRUCKER et al. 2008; SCHIETTI et al. 2014). Na Amazônia Central, por exemplo, florestas de platô (em altitudes maiores) apresentam lençol freático profundo (> 20 m de profundidade), potencialmente fora do alcance da maioria das espécies de árvores, enquanto as florestas de baixio (em altitudes menores) apresentam lençol freático superficial. Estudos prévios têm demonstrado que espécies associadas a habitats com lençol freático profundo apresentam características que conferem maior segurança hidráulica contra embolismos (estratégia comum em ambientes mais secos), enquanto espécies associadas a habitats com lençol superficial apresentam características que conferem condução mais eficiente (estratégia comum em ambientes mais úmidos) (COSME et al. 2017; OLIVEIRA et al. 2019; GARCIA et al. 2021, 2023).

Diferentes mecanismos ecofisiológicos podem determinar o padrão de integração que emerge da coordenação entre múltiplas características (KLINGENBERG 2014; MESSIER et al. 2017; PIGLIUCCI 2003). Demandas conflitantes (em inglês, *trade-offs*) na aquisição e uso da água e de outros recursos, por exemplo, podem gerar combinações inviáveis entre características funcionais. Além disso, restrições biofísicas, alométricas e evolutivas também podem afetar o padrão de integração funcional. Nesse contexto, têm-se demonstrado que a importância relativa desses diferentes mecanismos depende da escala e sistema de estudo considerados (MESSIER et al. 2017). Portanto, é de grande importância considerar as diferenças nas condições locais para entender os principais mecanismos que determinam a integração de características relacionadas ao uso da água nas plantas.

Dado que também temos pouca clareza se espécies associadas a habitats hidrologicamente contrastantes apresentam estratégias distintas de integração da sua

arquitetura hidráulica, aqui escolhemos os platôs e baixios da Amazônia Central como nosso sistema de estudo. Por um lado, espécies associadas com baixio (lençol superficial) devem ter um fácil acesso à água subterrânea, inclusive quando a precipitação cai abaixo de 100 mm durante os meses secos (COSTA et al. 2022), enquanto espécies associadas aos platôs (lençol profundo) poderiam sofrer mais intensamente com as secas sazonais. Se a menor disponibilidade de água no solo das florestas de lençóis freáticos profundos é um problema compartilhado por vários órgãos simultaneamente durante a estação seca, uma integração mais forte da arquitetura hidráulica deve ser favorecida nos platôs à medida que as plantas se desenvolvem e atingem o dossel da floresta. Pelo contrário, nos baixios a água não é um recurso limitante, embora essas áreas possam estar sujeitas a longos períodos de encharcamento do solo durante os meses chuvosos (COSTA et al. 2022). Nesse sentido, assumimos que as estratégias funcionais selecionadas sob excesso de água não devem ser restringidas por outras funções de uso da água e que tais condições devem permitir uma arquitetura hidráulica mais flexível (menos integrada) à medida que as plantas se desenvolvem e atingem o dossel nessas áreas.

OBJETIVO

Avaliar se características funcionais relacionadas ao uso da água estão integradas em uma rede de arquitetura hidráulica e avaliar quais as diferenças nos padrões de integração de espécies de dossel associadas a habitats hidrologicamente contrastantes (platô e baixio).

REFERÊNCIAS

BRODRIBB, Timothy J. Xylem hydraulic physiology: The functional backbone of terrestrial plant productivity. Plant Science, v. 177, n. 4, p. 245–251, 2009.

COSME, Luiza H. M. et al. The importance of hydraulic architecture to the distribution patterns of trees in a central Amazonian forest. New Phytologist, v. 215, n. 1, p.113–125, 2017.

COSTA, Flávia R. C. et al. The other side of tropical forest drought: do shallow water table regions of Amazonia act as large‐scale hydrological refugia from drought? New Phytologist, v. 237, p. 714–733, 2022.

CRUIZIAT, Peter et al. Hydraulic architecture of trees: main concepts and results. Annals of Forest Science, v. 59, n. 7, p. 723-752, 2002.

DAWS, Matthew I. et al. Topographic position affects the water regime in a semideciduous tropical forest in Panamá. Plant and Soil, v. 238, p. 79–89, 2002.

DEANS, Ross M. et al. Optimization can provide the fundamental link between leaf photosynthesis, gas exchange and water relations. Nature Plants, v. 6, p. 1116–1125, 2020.

DE CASTILHO, Camila V. et al. Variation in aboveground tree live biomass in a central Amazonian Forest: effects of soil and topography. Forest Ecology and Management, v. 234, p. 85–96, 2006

DRUCKER, Débora P. et al. How wide is the riparian zone of small streams in tropical forests? A test with terrestrial herbs. Journal of Tropical Ecology, v. 24, p. 65–74, 2008.

GARCIA, Maquelle N. et al. Local hydrological gradients structure high intraspecific variability in plant hydraulic traits in two dominant central Amazonian tree species. Journal of Experimental Botany, 2021.

KLINGENBERG, Christian P. Studying morphological integration and modularity at multiple levels: Concepts and analysis. Philosophical Transactions of the Royal Society B: Biological Sciences, v. 369, n. 1649, p. 33–35, 2014.

LAMBERS, Hans & OLIVEIRA, Rafael S. Plant Water Relations. In: Plant Physiological Ecology. Springer, Cham, 2020.

MCDOWELL et al. Drivers and mechanisms of tree mortality in moist tropical forests. New Phytologist, v. 219, n. 3, p. 851–869, 2018.

MESSIER, Julie et al. Trait variation and integration across scales: is the leaf economic spectrum present at local scales?. Ecography, v. 40, n. 6, p. 685–697, 2017.

OLIVEIRA, Rafael S. et al. Embolism resistance drives the distribution of Amazonian rainforest tree species along hydro-topographic gradients. New Phytologist, v. 221, n. 3, p. 1457–1465, 2019.

PIGLIUCCI, Massimo. Phenotypic integration: Studying the ecology and evolution of complex phenotypes. Ecology Letters, v. 6, n. 3, p. 265–272, 2003.

SCHIETTI, Juliana et al. Vertical distance from drainage drives floristic composition changes in an Amazonian rainforest. Plant Ecology & Diversity, v. 7, p. 241–253, 2014.

TYREE, Melvin T. & EWERS, Frank W. The hydraulic architecture of trees and other woody plants. New Phytologist, v. 119, n. 3, p. 345–360, 1991.

TYREE, Melvin T. & SPERRY, John S. Vulnerability of Xylem to Cavitation and Embolism. Annual Review of Plant Physiology and Plant Molecular Biology, v. 40, n. 1, p. 19-36, 1989.

CAPÍTULO ÚNICO

Height-related hydraulic constraints drive a tighter integration of the hydraulic architecture of canopy trees in Central Amazonia

Manuscrito submetido à revista *New Phytologist*.

Height-related hydraulic constraints drive a tighter integration of the hydraulic architecture of canopy trees in Central Amazonia

Matheus G B Rosa, Luiza H M Cosme, Mirza L Bezerra, Juliana Schietti

Abstract

- Soil water availability has a significant impact on the plant phenotype. However, it is unclear whether plant traits related to water use can be integrated into a unified hydraulic architecture across plant organs.
- We analyzed the interspecific trait correlation network of 11 functional traits related to water use in 28 canopy tree species associated with valleys and plateaus in Central Amazonia.
- Taller trees had fewer wider vessels and a thicker bark in their terminal branches, their leaves had lower SLA, with fewer wider stomata, and their trunks invested in proportionally less sapwood area than shorter species. Plateau species, in particular, exhibited a stronger integration pattern, with high clustering of tree height, bark thickness, and vessel and stomatal traits in the trait correlation network, while valley species displayed a more sparsely connected network with no specific trait or set of traits holding more relative importance in the network topology.
- Our results suggest that height-related constraints integrate water and carbon use in the canopy trees of a Central Amazonian forest, and that species adapted to drier conditions (plateaus) exhibited a more tightly integrated hydraulic architecture than those adapted to wetter conditions (valleys) in a Central Amazonian forest.

Keywords. canopy trees, functional integration, hydraulic architecture, trait correlation network, tropical rainforest.

Introduction

Plant water relations are central to understanding the diversity and distribution of tropical trees and how they might respond to a changing environment (Oliveira *et al.*, 2021; Costa *et al.*, 2022; Marca-Zevallos *et al.*, 2022; Sousa *et al.*, 2022). Through the differential allocation of resources across plant organs and within tissues, plants can adjust the structure of their water transport system in response to soil water availability (Cosme *et al.*, 2017; Rosas *et al.*, 2019). For instance, drier environments often select individuals and species with xylem traits that confer higher resistance to embolisms than wetter environments (Oliveira *et al.*, 2019; Fontes *et al.*, 2020; Garcia *et al.*, 2021), including traits such as smaller vessels and denser sapwood (Cosme *et al.*, 2017). Besides these effects on the xylem, environmental water availability can also impact different plant organs through direct or indirect effects on how plants transport water, regulate water loss, or store water in their tissues (Bucci *et al.*, 2004; Pratt & Jacobsen, 2017; Tng *et al.*, 2018). Drought-induced decreases in water potential, for example, can both trigger stomatal closure and push for the release of water stored within tissues back into the hydraulic pathway, thus compensating for high xylem tensions and decreasing the risk of embolisms (Poorter *et al.*, 2014; Pratt & Jacobsen, 2017; Lambers & Oliveira, 2020). Thus, it is of great importance to study plant hydraulic architecture considering the integration of water conduction, loss, and storage across multiple organs, to effectively describe how local hydrological conditions affect plant functioning.

Trait-based ecology has made significant progress in understanding how trade-offs constrain functional variation and how such constraints result in the coordinated response of multiple traits in the phenotype (Westoby *et al.*, 2002; Reich *et al.*, 2003; Wright *et al.*, 2004; Díaz *et al.* 2016). The Leaf Economics Spectrum, for example, describes a worldwide trend in leaf trait variation based on the trade-off between leaf productivity and longevity, ranging from highly productive low-cost leaves on the acquisitive side of the spectrum to long-lived high-cost leaves on the conservative side (Wright *et al.*, 2004). Similarly, some authors have proposed a Wood Spectrum based on the predicted trade-offs among transport efficiency, embolism resistance and mechanical support (Baas *et al.*, 2004; Chave *et al.*, 2009), because most xylem traits associated with a highly efficient water transport system usually compromise the stem's ability to withstand mechanical and hydraulic stresses. In both contexts, different plant functional traits have been linked to life history strategies (Poorter & Bongers, 2006; Poorter *et al.*, 2010; Oliveira *et al.*, 2021), with slow-growth species often showing more conservative leaves and/or safer hydraulic architecture than fast-growth

species. Considering that life history strategies are determined by the overall plant phenotype, and that resource allocation in one part of the plant may also reflect resource allocation in other parts, a whole-plant economics spectrum has been suggested based on the coordination of multiple plant organs within a common 'fast-slow' trade-off framework (Reich, 2014). However, it remains unclear whether and how the relationships among multiple traits at local scales in fact reflect worldwide trait dimensions (Messier *et al.*, 2017a).

Biophysical rules, evolutionary constraints, and environmental factors are important drivers of trait correlations among species, and the relative strength of these mechanisms may differ across scales resulting in different integration patterns (Reich *et al.* 2003; Messier *et al.*, 2017a). While some trait correlations reflect hard constraints that are almost impossible to avoid and are consistent across scales, such as those following strict biophysical and allometric rules, others may reflect soft constraints that vary across scales and different selective pressures (Messier *et al.* 2017a; Pratt & Jacobsen 2017). Hence, to have a clear understanding of the drivers of plant phenotypic integration at a specific spatial scale, one must account for differences in environmental conditions.

Recently, a shift from trait dimensions towards a network perspective in studying the relationships among multiple traits has been advocated, as graph theory provides useful tools for analyzing trait correlation matrices (Messier *et al.*, 2017b; Kleyer *et al.*, 2018; Messier *et al.*, 2018; Flores-Moreno *et al.*, 2019; Rosas *et al.*, 2019; Burton *et al.*, 2020; Carvalho *et al.*, 2020; He *et al.*, 2020; Benavides *et al.*, 2021; Liu *et al.*, 2022). By using functional traits as nodes in a network and correlations between traits as links between nodes, it is possible to graphically represent the phenotype as a trait correlation network, making it easy to understand how different parts of the organism connect to each other. Besides, one can also study the structure of trait correlation networks and quantify topological properties as a proxy for phenotypic integration patterns (Messier *et al.*, 2017b; Benavides *et al.*, 2021).

Trait integration patterns have been analyzed across various spatial and biological scales, as well as environmental gradients, using trait correlation networks (Flores-Moreno *et al.*, 2019; Rosas *et al.*, 2019; Carvalho *et al.*, 2020; Benavides *et al.* 2021). In this context, some authors argue that harsh environmental conditions select for more tightly integrated phenotypes, as evidenced by the higher trait integration in European Pine populations subjected to harsh local conditions, and the increasing integration in populations towards higher latitudes (Carvalho et al., 2020; Benavides et al., 2021). Their argument is based on the

assumption that an increased coherence among traits favors an optimal response to environmental stresses. Others, on the contrary, argue that the flexibility of combining traits in multiple ways enables rapid adjustments of plant function to cope with harsh conditions (Flores-Moreno *et al.*, 2019; Rosas *et al.*, 2019). In any case, a trait integration pattern is the result of selective pressures acting on multiple traits with a shared function, either driving a stronger or weaker coordination among traits.

Our study system is characterized by a topographic gradient with plateaus on the top of ridges and *'baixios'* on the bottom of valleys along riparian areas, showing marked changes in vegetation structure and species composition at local scales (de Castilho *et al.*, 2006; Drucker *et al.*, 2008; Schietti *et al.* 2014). Topographic position is also an important driver of differences in soil-water conditions (Daws *et al.*, 2002). Plateau forests, for instance, can have a water table deeper than 20 m, potentially out of reach for most tree species, whereas valley forests have a shallower water table very close up to the surface (Drucker *et al.*, 2008). Because valleys have a shallow water table easily accessible when precipitation falls below 100 mm during the dry months (Costa *et al.*, 2022), we argue that canopy species associated with plateaus should experience seasonal droughts more intensely than species associated with valleys. As the shortage of water in deep water table forests becomes a shared problem for multiple organs simultaneously during the dry season, a tighter integration of the hydraulic architecture should be favored in plateaus as plants develop and reach the canopy. Valleys on the contrary should have plenty of water in the soil throughout the year, including the dry months, though these areas can be subjected to long periods of waterlogging during the rainy months (Costa *et al.*, 2022). Assuming that water is not a limiting resource in waterlogged habitats, we argue that the functional strategies selected under water excess should not be constrained by other water-use functions, thus allowing a more flexible (less tightly integrated) hydraulic architecture as plants develop and reach the canopy in valley forests.

Here, we focused on 11 functional traits related to water-use in the stem, branches, and leaves of 28 canopy species in Central Amazon and asked: (i) are these plant traits functionally integrated into a unified hydraulic architecture network?; (ii) do species associated with contrasting soil-water conditions have different integration patterns of their hydraulic architecture network? Given the intricate relationships between water conduction, loss, and storage, we expected that trees would have a functionally integrated hydraulic architecture, with the coordination of multiple traits in the phenotype reflecting a whole-plant

water-use strategy. We also expected that species associated with drier conditions would show a more tightly integrated hydraulic architecture than species associated with wetter conditions.

Methods

Study area

The study was conducted at Reserva Florestal Adolpho Ducke of the Instituto Nacional de Pesquisas da Amazônia (Ducke Reserve, INPA), based on the database collected by Cosme et al., 2017. Located north of Manaus in the central region of the Amazon basin, the Ducke Reserve covers 10 000 ha of tropical rainforest, with a canopy height of 30-37 m and an overstory that can reach up to 45 m (Ribeiro *et al.*, 1999). The mean annual rainfall from 1966 to 2016 was around 2 500 mm (Esteban *et al.*, 2021). August was the driest month with an average precipitation of 98 mm, but the dry season (with precipitation < 100 mm) can extend from July to September in some years (Esteban *et al.*, 2021). August had a historical mean temperature of 26 ºC and April (the wettest month) of 25.2 ºC (Esteban *et al.*, 2021).

Traits

We focused on 11 plant anatomical and morphological traits related to water-use (Table 1), including bark and stomatal traits that were not previously published in Cosme *et al.* (2017). Trait sampling was conducted between 2014 and 2015 in 158 adult canopy trees of 28 species from the six most abundant families at the Ducke Reserve (Table 2). For each pair of species, one was mostly associated with *baixios* (hereafter valley species), and the other was mostly associated with plateaus and higher slope areas (hereafter plateau species) (Table 2) (Cosme *et al.*, 2017). The species selection criterion used by Cosme et al. (2017) involved sampling of congeneric species linked to differing soil-water conditions. This allowed assessment of habitat segregation among closely related species. Name revisions did not affect the close evolutionary relationships between the selected species pairs.

To determine stem structural traits, we obtained wood samples with a diameter of 5.15 mm and a length equal to the trunk radius at 1.2 m above the ground, using a Pressler's borer. Wood density (WD) was calculated as the dry weight per fresh volume (g cm^{-3}) of the first 5 cm of the core sample, excluding the bark. WD reflects plant carbon allocation to structural tissues and it is often thought of as a central trait in the hydraulic architecture linking the trade-offs of hydraulic efficiency, embolism resistance, and mechanical support (Baas *et al.*,

2004; Chave *et al.*, 2009). Stem sapwood area was determined by positioning a strong light source against the fresh core sample and measuring the portion of the wood that allowed the passage of light. With this measure, the sapwood area to basal area ratio (As:Ba) was determined to describe the proportion of active xylem in the stem relative to the trunk cross-sectional area.

With the assistance of experienced climbers, sun-exposed branches with fully expanded leaves were collected from the upper canopy, and tree height (H) was measured (Cosme *et al.*, 2017). With the branch samples, we determined 4 structural traits and 4 anatomical traits. Bark thickness (BT) was estimated as half of the difference between the total branch diameter and the branch diameter without bark, and bark density (BD) was estimated as dry weight per fresh volume of the difference between the whole sample and the sample without bark. Thicker and less dense barks retain more water, possibly increasing resistance to hydraulic failure as the water stored in their tissues becomes available under high xylem tension (Poorter *et al.*, 2014). Specific leaf area (SLA) was determined as the ratio between the mean fresh leaf area and mean dry weight in two selected leaves of the branch. Leaves with high values of SLA are associated with higher photosynthetic rates (Wright *et al.*, 2004) and thus can be linked to higher evapotranspiration demand. Leaf area in the branch was measured by scanning all leaves of the branch (without petiole) and branch sapwood area was determined by subtracting pith area from the total branch cross-sectional area after the bark was removed. These two latter were then used to determine the branch Huber value (Hv), *i.e.* the ratio between branch sapwood area and leaf area in the branch, which is the inverse ratio of $A_l:A_{s(branch)}$ included in Cosme *et al.* (2017). Hv describes the allocation of water supply per unit of water demand (Rosas *et al.*, 2019).

We considered two vessel anatomy traits related to water conduction in the branch xylem. The hydraulically weighted mean vessel diameter (Dh) and vessel density (VD) were measured in subsamples collected in at least one individual of each species. To determine these traits, xylem cross-section of 15-40 μm thick were fixed and photographed (see Cosme *et al.*, 2017 Materials and Methods for further details). VD was measured as the number of vessels in an area of 352 cm². Individual vessel diameter was estimated by the individual vessel area measured in the photographs as $D_i = (4A_i/\pi)^{½}$, and the hydraulically weighted mean vessel diameter was determined as $Dh = \Sigma D_i^5/\Sigma D_i^4$. Because of this direct mathematical link, Dh is almost perfectly correlated with mean vessel area ($r = 0.989$, $p < 0.001$).

We also considered two stomatal anatomy traits, because stomata are key structures driving the coordination of water loss, photosynthesis, and water conduction (Rosas *et al.*, 2019; Deans *et al.*, 2020; Simioni *et al.*, 2023), by regulating the gas exchanges between the leaf and the atmosphere. To determine stomatal density (SD) and stomatal pore length (SL), a proxy for stomatal size (de Boer *et al.*, 2016), we dissociated the leaf epidermis following the Franklin 1945 procedure (modified by Kraus & Arduin, 1997). Next, the epidermis was peeled off of the leaves, stained with 1% safranin, mounted in a microscope slide and photographed in an optical microscope (Leica DM500, Leica Microsystems, Wetzlar, Germany) at ×200 magnification. The photographs were analyzed with ImageJ (https://imagej.nih.gov/ij/). SD and SL were determined for 26 of the 28 species because all samples from *Leptobalanus longistylus* and *Leptobalanus octandrus* were fragmented in the dissociation procedure.

Partition of variation

Using the individual measures, we fitted intercept-only linear mixed models for each trait (trait = 1 + (1 | genus) + (1 | genus:species) + Residuals) to determine how much trait variation was due to genus and interspecific differences (Harrison *et al.*, 2018; Emilio *et al.*, 2021). Model parameters were estimated with the *lmer* function in the *lme4* package. Total explained variance equals the sum of among genus, among species and residual variance, and variation was partitioned by calculating the proportion of variation explained by each random factor (genus and species) and the unexplained residuals. Before all analyses, we checked for extreme values in trait distribution and removed them from the data (see Notes S1).

Interspecific trait coordination

We estimated interspecific pairwise trait coordination using Pearson's correlations of species means. We also tested whether the relationships between pairs of traits had different slopes depending on the soil-water conditions. We did so by modeling the interaction between species habitat and one of the traits (trait 1 ~ trait 2 * habitat).

Network analysis

To assess the functional integration pattern among plant traits related to water-use, we computed functional traits as nodes in a network and the significant correlations between pairs of traits as links between nodes. To do so, first we computed a correlation matrix using the

rcorr function in the *Hmisc* package, and from that we defined a binary adjacency matrix by setting p-values ≤ 0.05 to 1 (significant r) and p-values > 0.05 to 0 (non-significant r), and a weighted adjacency matrix by multiplying the binary adjacency matrix to the absolute values of the original correlation matrix. Then, we generated undirected unipartite graphs using the *graph_from_adjacency_matrix* function. We followed this procedure with the pooled data and with plateau and valley species separately to assess the differences across contrasting habitats. Network analysis was conducted in the igraph package (Csardi & Nepusz, 2006).

Using the binary correlation network, we computed the number of significant correlations of each trait (*i.e.* node degree), and the ratio of significant correlations relative to the maximum number of possible trait combinations (*i.e.* the edge density of the whole network – ED) . ED is determined for the whole network by the following equation:

$$ED = \frac{2L}{N(N-1)} \qquad \textit{eq. 1}$$

where L is the number of links observed in the network and N is the number of nodes. If *ED* = 0, the network is completely disconnected, whereas if *ED* = 1, the network is completely connected. This way, *ED* can be interpreted as the probability that two randomly drawn traits are significantly correlated. While *ED* describes the connectivity structure of the whole network, node degree is a centrality measure at the level of individual nodes that describes the number of connections with other nodes in the network (Barabási, 2016).

To describe the dispersion and clustering of nodes in the network, we calculated the average distance and the average clustering. To measure the distance between two nodes in a network, one calculates the minimum number of links necessary to leave one node and reach another (*i.e.* the shortest path length). This way, the average distance in a network (*i.e.* the average shortest path length) describes how much the nodes are away from each other (Barabási, 2016). On the other hand, the clustering coefficient of a node is a measure of the connectivity between the neighbors of that node, and is calculated by the following equation:

$$C_i = \frac{2L_i}{k_i(k_i-1)} \qquad \text{eq. 2}$$

where L_i represents the number of links between the k_i neighbors of node *i*. If $C_i = 0$, none of the neighbors (k) of node *i* link to one another, whereas if $C_i = 1$, all of the neighbors of node *i* link to one another. This way, the average clustering of a network can be interpreted as the

probability that a trait in the network links to already linked traits (Barabási, 2016). Only connected nodes have measures of distance and only nodes with a minimum of two neighbors have measures of clustering, hence disconnected and peripheral nodes do not affect the network's average distance and clustering because they return Inf or NA.

Random network model

To test whether the properties of valley and plateau networks differed from randomness, we simulated random networks with the G (N, L) Erdős–Rényi model. In the G (N, L) random network model, the number of nodes N and the number of links L were fixed according to the values of the observed network, and random networks were generated with the same edge density as the observed network (Barabási, 2016). We then computed the average distance and average clustering for 999 randomly wired networks and summarized the distributions by their means and standard deviations. With this, we calculated the standardized effect size of these measures by the following equation:

$$ses = \frac{obs - mean(null)}{sd(null)} \qquad \textit{eq. 3}$$

where *ses* > 0 indicates that the average distance or the average clustering of the observed network is higher than of random networks with the same edge density, while *ses* < 0 indicates lower distances or clustering values.

Phylogenetic relatedness

To account for the phylogenetic relationships among species, we updated a phylogeny for the 28 species here included (figS5) using the backbone GBOTB.extended.TPL in the *V.PhyloMaker2* package (Jin & Qian, 2022; Smith & Brown, 2018). The updated phylogeny still supported the close evolutionary relationships between the selected species pairs (Table 2; Fig S5). First, we computed Pagel's λ (Pagel, 1999) with the function *phylosig* in the *phytools* package to assess the phylogenetic signal of each trait (Revell, 2012). Pagel's λ is a scalar parameter that transforms the branch distances in the phylogeny to better fit a Brownian motion model of trait evolution. When Pagel's $\lambda = 1$, the untransformed phylogenetic distances are the better predictor of trait variance under a Brownian motion model, while values of $0 < \lambda < 1$ indicate that the phylogenetic distances must be downweighted to better fit a Brownian motion model. In contrast, for $\lambda = 0$, the phylogenetic distances are all set to

zero and species are considered independent of one another as they would be in an ordinary least squares model.

To assess the phylogenetic trait correlation network, first we computed the trait covariance matrix assuming a given λ with the *phyl.vcv* function in the *phytools* package, then we scaled the resulting trait covariance matrix into a trait correlation matrix using *cov2cor* function, and tested whether each phylogenetic trait correlation differed from zero using the t-statistics distribution. After that, we repeated the steps presented in the Network Analysis section. For this procedure, we removed species with missing data (*Leptobalanus longistylus* and *Leptobalanus octandrus*) because we needed a complete matrix. Also, because all of our traits showed $\lambda < 1$ (Table S2), and almost half of our traits did not show a significant λ, we repeated this analysis for 4 different scenarios: $\lambda = 0$, λ = our mean lambda, λ = our maximum lambda, $\lambda = 1$. Through this we assessed the phylogenetic trait correlations at more conservative λ to avoid overestimating the effects of phylogenetic relatedness in our trait correlations.

Results

In most traits, genus and species identity explained more than 50% of individual variation (Fig. 1). Wood density was the least plastic trait with the highest proportion of variation explained by the sum of among genus and among species variances (85.21%), and Huber value was the most plastic trait with only 10.54% of its variation being explained by genus and species identity (Fig. 1). Wood density was also the most phylogenetically conserved trait (Pagel's $\lambda = 0.77$, $p < 0.001$). Bark density, tree height, specific leaf area and vessel density also showed significant phylogenetic signal (Table S2), while stomatal density had a marginally significant phylogenetic signal (Pagel's $\lambda = 0.347$, $p = 0.066$).

The 11 functional traits here considered were all connected into a single trait correlation network when we pooled valley and plateau species together (Fig. 2). Tree height and vessel density were the most central traits in this network with 7 significant correlations out of 10 possible pairs, followed by SLA with six, whereas Hv was the most peripheral trait significantly correlated to SLA alone (Fig. 4a). The five traits with the highest degrees (VD, H, SLA, As.Ba and Dh) formed a fully connected subgraph in the network, *i.e*, a *clique*. In addition, there were two triangles (*cliques* of three vertices) determined by positive correlations only and they were linked to one another by negative correlations. The stronger

positive-only triangle was formed by H, Dh and SL, traits related to plant and cell sizes, and the weaker triangle was formed by VD, SLA and As.Ba, traits describing carbon allocation within leaves and xylem (Fig. 2).

When valley and plateau species were considered separately, we found that some traits were not connected to the network's larger component. In the valley network, bark thickness was disconnected from the network, and so was the stomatal pair SL and SD (Fig. 3a). In the plateau network, both the Huber value alone and the pair As.Ba and WD were disconnected from the larger component (Fig. 3b). In addition, the valley network was characterized by a much sparser topology than the plateau network. In the valley network, SLA, WD, As.Ba, VD and Dh had three significant correlations with other traits (Fig. 4b), which was the maximum degree in this network. In the plateau network, tree height was the most central trait in the network (Fig. 4c), and formed a *clique* with Dh, SL and VD (Fig. 3b).

In the pooled network, we observed 23 significant correlations out of 55 possible links, yielding an $ED = 0.42$ (Table 3). Positive correlations varied from 0.39 to 0.73, while negative correlations varied from -0.75 to -0.39 (Fig. S1). In the valley and plateau networks, we observed 11 and 13 links, $ED = 0.2$ and $ED = 0.24$, respectively (Table 3). Only three links were common to both valley and plateau networks: H-Dh, SL-SD, and As.Ba-WD (Fig. 3; Fig. S2). From these shared links, only the relationship between tree height and vessel diameter showed a significant interaction with species habitat, where plateau species had a steeper slope than valley species (Fig. S3a). However, this steeper relationship between H-Dh among plateau species was forced by the tallest species in the dataset – *Cariniana micrantha*, a deciduous species associated with plateaus. Removing this species from the model resulted in a non-significant interaction with species habitat (data not shown). Other three relationships (WD-VD, BT-VD and Hv-As.Ba) showed a significant interaction with species habitat, but the relationship was significant in only one of the habitats and not in the other (Fig. S3b-d). The relationships between WD-VD and between Hv-As.Ba were only found among valley species but not plateau species (Fig. S3b,d), while the relationship between BT-VD was only found among plateau species (Fig. S3c). Relationships with tree height for the pooled data are highlighted in Fig. 5, most of these relationships were also strong among plateau species, except for the links between H-SLA and H-As.Ba which were not found in the plateau network because their p-values were only marginally significant ($p = 0.06$, data not shown).

The plateau network was more clustered than the valley network, but the average distance did not differ much (Table3). In the valley network, the average distance was 1.86 links and in the plateau network 1.93 links, while the average clustering of the valley network was 0.35 and of the plateau network 0.6 (Table 3). Finally, we tested whether the average distance and clustering of valley and plateau networks were different from random expectation (Fig. 6). We found that, after accounting for differences in edge density, the average distance of valley and plateau networks were usually lower than the random mean, but fell completely inside the interval explained by chance alone (Fig. 6a,b). On the other hand, the average clustering of the plateau network was 3.3 sd units above the random mean where random networks rarely reach, but that of the valley network fell completely inside the random expectation (Fig. 6c,d). Thus, the plateau network was more clustered than random networks while the valley network was not.

In the phylogenetic trait correlation networks across different values of Pagel's λ, we showed that tree height remained a central trait in the network, except when λ = 1 (Fig S6). We also showed that most links in the network with λ = 1 were negative correlations between traits, indicating that most trade-offs were consistent when we overestimated the effect of phylogenetic relatedness on trait relationships. Particularly, the negative correlations between VD and Dh, SL and SD, and WD and As.Ba, were common to all networks here analyzed (Fig. S4, S6). The relationships between H-Dh and H-SLA were also consistent across all λ scenarios (Fig. S6), despite the high phylogenetic signals of H and SLA (Table S2). Removing the two species with missing data to perform this analysis did not affect the original network topology as just one link (BD-BT) was missing in the resulting network (Fig S6a).

Discussion

Tree height is a highly integrative trait in the hydraulic architecture of canopy trees in this study system, linking xylem vessel and stomatal anatomy to leaf, stem, and bark structure. In general, taller species in the canopy had fewer and larger vessels, fewer stomata and larger stomatal pores, thicker bark, low SLA leaves, and low proportions of sapwood area in the stem. Such relationships support the theory that height-related constraints tightly couple the water and carbon use across plant organs (Ryan & Yoder 1997; Ryan *et al.*, 2006; Reich, 2014; Fernández-de-Uña *et al.*, 2023).

We also showed that the hydraulic architecture network of valley and plateau species displayed different topologies, suggesting that local hydrology might select different integration of water-use traits as species adapt to contrasting extremes of a topographic gradient. The hydraulic architecture of plateau species exhibited tight correlations among tree height, vessel and stomatal anatomy, and bark thickness, whereas that of valley species did not. As expressed by the high average clustering of the plateau network, traits related to water conduction, loss, and storage were strongly integrated among plateau species. Furthermore, the disconnected traits within the plateau network were primarily associated with mechanical functions, suggesting a loose connection between tree hydraulics and mechanical support among plateau species. Contrastingly, among valley species, tree height was linked only to vessel diameter and SLA, while stomatal traits and bark thickness were disconnected from the rest of the network. In this case, we suggest that although waterlogging can impose severe environmental stresses, including soil anoxia and low pH levels, in our study site, these conditions do not lead to a tighter integration of water-use-related traits. Instead, several distinct sets of traits appeared more sparsely organized without a central integrative trait.

Although there were differences in network topology, only four trait-trait relationships showed significant interaction with species habitat, indicating that in most trait relationships the general trend was consistent in both valley and plateau forests. In the cases where an interaction with species habitat was observed, we showed that bark thickness scaled with vessel density (- relationship) only among plateau species, whereas wood density scaled with vessel density (-) and the Huber value scaled with the proportion of sapwood (-) only among valley species. These relationships suggest that the close link between water storage and water conduction was only significant for plateau species, while the close link between mechanical support and water conduction was only significant for valley species. Taking these interactions into account, we must acknowledge that most differences observed between valley and plateau networks could be attributed to slight differences in correlation strength, rather than directionality. In addition, although we studied fewer species compared to larger global datasets containing hundreds of species, still we found that certain fundamental trade-offs remain remarkably consistent across spatial scales.

The hydraulically-weighted mean vessel diameter (Dh) consistently increased as tree height (H) increased. Although valley species had on average wider vessels than their closely-related plateau species (Cosme *et al.*, 2017), taller species in both habitats tended to have wider vessels than shorter ones. As trees grow taller, they must make many structural

adjustments to compensate for the increased resistance to water flow. Investing in wider vessels seems to counteract the higher resistance associated with longer conductive paths since xylem hydraulic conductivity is directly proportional to vessel radius raised to the fourth power in Hagen-Poiseuille's law (Tyree & Ewers, 1991; Olson *et al.*, 2014). Many studies have shown that taller plants have wider vessels at the tip of their branches, regardless of environmental conditions (Olson & Rosell, 2013; Olson *et al.*, 2014; Fajardo *et al.*, 2020). Conversely, climate also contributes significantly to worldwide vessel diameter variation by constraining maximum plant height (Hacke *et al.*, 2017; Rosell *et al.*, 2017). We found that the relationship between tree height and vessel diameter was steeper among plateau species and that this interaction with species habitat was mainly due to the strong effect of the tallest species in the data – *Cariniana micrantha*, a deciduous species associated with plateau areas. Thus, we can conclude that taller trees have wider vessels due to allometric scaling rules, being a hard biophysical constraint (*sensu* Messier *et al.*, 2017a), but at local scales, this relationship can be steeper depending on the habitat and species functional strategies.

Stomatal density and pore length were inversely related among valley and plateau species, consistent with the trade-off principle of optimizing leaf area for gas exchange area (de Boer *et al.*, 2016). Both the number and size of stomata in the leaf epidermis allow plants to adjust their gas exchange rates (Drake *et al.*, 2013). In this context, it has been shown that stomata with larger guard cells have lower conductance rates and slower responsiveness, whereas stomata with smaller guard cells have higher conductance rates and faster responsiveness (Drake *et al.*, 2013). This is because larger guard cells take longer to respond to changes in leaf water potential and their deeper pores increase the distance for gas diffusion (de Boer *et al.*, 2016; Xiong & Flexas, 2020). However, although longer guard cells tend to have longer pores (Drake *et al.*, 2013), it has also been shown that increasing stomatal pore length increases stomatal conductance rates by increasing the surface area available for gas exchange (Aasamaa *et al.*, 2001). Our results show that taller species in the canopy had fewer stomata in their leaves but with longer pores, which may indicate stomata with higher conductance rates and slow responsiveness. Further studies are needed to clarify whether different anatomical measures of stomatal size (*e.g.*, guard cell length and width, stomatal pore length and depth) have the same effect on the transpiration rate, and how tree height relates to these measures.

We also found that stomatal pore length was directly correlated with vessel diameter, a relationship that may be explained by genetic constraints on cell size. Genome size is a strong

predictor of cell size, driving the coordination of larger vessels with larger stomata, larger epidermal cells, higher leaf thickness, and overall larger cell sizes in Proteaceae species and across angiosperm taxa (Brodribb *et al.*, 2013; Jordan *et al.*, 2015). However, this mechanism cannot explain the scaling of vessel and stomatal anatomy with tree height, as we found no evidence of genome size determining tree height variation.

Trees that reach the forest canopy top are exposed to high vapor pressure deficits, high solar radiation, and strong winds (Gora & Esquivel-Muelbert, 2021), factors that lead to higher canopy-wide evapotranspiration rates. Because high xylem tension increases the risk of hydraulic failure due to vascular cavitation and embolism (Oliveira *et al.*, 2019), plants must compensate for the hydraulic constraints associated with regulating water loss, especially during drought when both atmospheric relative humidity and soil water availability are very low. The hydraulic limitation hypothesis states that once trees have grown to their maximum height, they become limited in their further growth by stomatal control (Ryan & Yoder, 1997). This is primarily because the stomata of taller trees close earlier in the day (Yoder *et al.*, 1994) to prevent the increase of xylem tensions to levels that could impair the hydraulic system, thereby limiting photosynthesis to a shorter period. Taken together, taller trees invest in wider vessels only to compensate for the vertical resistance to flow associated with tree height, but their leaves cannot sustain higher assimilation rates and faster resource turnover (Fernández-de-Uña *et al.* 2023). In accordance with the hydraulic limitation hypothesis, our results also support that taller plants have more conservative leaves than shorter ones (Ryan & Yoder, 1997; Liu *et al.* 2010; Fernández-de-Uña *et al.*, 2023).

Another short-term mechanism to buffer increases in xylem tension is the release of water stored in leaf, wood, and bark tissues (Phillips *et al.*, 2003; Poorter *et al.*, 2006). Taller plants appear to rely more heavily on water stored in their living tissues, especially when exposed to high solar radiation (Goldstein *et al.*, 2002; Phillips *et al.*, 2003). We showed that bark thickness increased with tree height among plateau species, potentially allowing for greater water storage capacity as trees grow taller. Other traits, however, (e.g. wood density) may also influence water storage capacity and be rather independent of tree height.

Wood density has been linked to water storage capacity and drought resistance, but in our study wood density was not an integrative trait in the hydraulic architecture of canopy species. It is expected that denser wood should be more resistant to xylem implosion at very negative water potentials, allowing the xylem to withstand drier conditions (Hacke *et al.*,

2001). Indeed, previous studies have shown that plateau species have higher resistance to embolism than valley species (Oliveira *et al.*, 2019), and that plateau species have denser wood than their closely-related valley species (Cosme *et al.*, 2017), suggesting that plateau species may invest in higher safety against embolism by increasing wood density. Another important mechanism for the relationship between wood density and drought resistance is that denser wood can withstand lower limits in water potential and resist longer against the negative effects of drought on cell turgor, as demonstrated by the lower turgor loss point and lower osmotic potential at full turgor of dense woods (Santiago *et al.*, 2018). In contrast, Santiago *et al.*, (2018) also showed that denser wood had lower sapwood water capacitance and lower saturated water content, traits that describe low water storage capacity at the tissue level. Our findings thus suggest that plants can invest in safer wood independently from water transport efficiency and that a trade-off between drought tolerance and water storage capacity may be stronger and more closely related to wood density variation than the weak trade-off between drought tolerance and water conduction efficiency (Gleason *et al.*, 2016; Pratt & Jacobsen, 2017). Future studies could address the relationship between tree height, water storage capacity, and drought resistance more directly, by including traits such as the proportion and distribution of parenchyma cells (Morris *et al.*, 2018) or by evaluating water content, osmotic potential, and turgor loss point across plant tissues (Santiago *et al.*, 2018).

In this study, we examined interspecific trait correlation networks across plant organs to gain insights into the multiple trade-offs and constraints that shape the integration of water conduction, loss, and storage in species associated with contrasting hydrological conditions in a Central Amazonian forest. We showed that tree height is a very important trait that integrates leaf, bark and wood when pooling both plateau and valley species. We also showed that the average clustering of the trait correlation network can vary significantly under different hydrological conditions. The plateau network was highly clustered, whereas the valley network had a more dispersed topology with properties that were not different from random. The higher clustering found in the plateau network implies that further constraints on height growth may also have strong effects on the vessel, stomatal, and bark structure of plateau species. This suggests that increasing drought regimes would impose stronger constraints on the phenotype of plateau species than on valley species. However, studies evaluating intraspecific patterns of variation and phenotypic integration are needed to shed light on how specific populations may respond to their environmental conditions. Such studies could also help us predict how the plant phenotype shall respond to climate change.

References

Armbruster WS, Pélabon C, Bolstad GH, Hansen TF. **2014**. Integrated phenotypes: understanding trait covariation in plants and animals. *Philosophical Transactions of the Royal Society B: Biological Sciences* **369**: 20130245.

Aasamaa K, Sõber A, Märt R. 2001. Leaf anatomical characteristics associated with shoot hydraulic conductance, stomatal conductance and stomatal sensitivity to changes of leaf water status in temperate deciduous trees. *Functional Plant Biology* **28**, 765-774.

Baas P, Ewers FW, Davis SD, Wheeler EA. **2004**. Evolution of xylem physiology. **In:** Hemsley AR, Poole I, eds. *The Evolution of Plant Physiology*. Elsevier, 273–295.

Barabási AL. **2016**. *Network Science*. Cambridge University Press.

Benavides R, Carvalho B, Matesanz S, Bastias CC, Cavers S, Escudero A, Fonti P, Martínez‐Sancho E, Valladares F. **2021**. Phenotypes of Pinus sylvestris are more coordinated under local harsher conditions across Europe. *Journal of Ecology* **109**: 2580–2596.

de Boer HJ, Price CA, Wagner‐Cremer F, Dekker SC, Franks PJ, Veneklaas EJ. **2016**. Optimal allocation of leaf epidermal area for gas exchange. *New Phytologist* **210**: 1219–1228.

Brodribb TJ, Jordan GJ, Carpenter RJ. **2013**. Unified changes in cell size permit coordinated leaf evolution. *New Phytologist* **199**: 559–570.

Bucci SJ, Goldstein G, Meinzer FC, Scholz FG, Franco AC, Bustamante M. **2004**. Functional convergence in hydraulic architecture and water relations of tropical savanna trees: from leaf to whole plant. *Tree Physiology* **24**: 891–899.

Burton JI, Perakis SS, Brooks JR, Puettmann KJ. **2020**. Trait integration and functional differentiation among co‐existing plant species. *American Journal of Botany* **107**: 628–638.

Camargo MAB, Marenco RA. **2011**. Density, size and distribution of stomata in 35 rainforest tree species in Central Amazonia. *Acta Amazonica* **41**: 205–212.

Carvalho B, Bastias CC, Escudero A, Valladares F, Benavides R. **2020**. Intraspecific perspective of phenotypic coordination of functional traits in Scots pine. *PLOS ONE***15**: e0228539.

de Castilho CV, Magnusson WE, de Araújo RNO, Luizão RCC, Luizão FJ, Lima AP, Higuchi N. **2006**. Variation in aboveground tree live biomass in a central Amazonian Forest: effects of soil and topography. *Forest Ecology and Management* **234**: 85–96.

Chave J, Coomes D, Jansen S, Lewis SL, Swenson NG, Zanne AE. **2009**. Towards a worldwide wood economics spectrum. *Ecology Letters* **12**: 351–366.

Cosme LHM, Schietti J, Costa FRC, Oliveira RS. **2017**. The importance of hydraulic architecture to the distribution patterns of trees in a central Amazonian forest. *New Phytologist* **215**: 113–125.

Costa FRC, Schietti J, Stark SC, Smith MN. **2022**. The other side of tropical forest drought: do shallow water table regions of Amazonia act as large‐scale hydrological refugia from drought? *New Phytologist* **237**: 714–733.

Csardi G & Nepusz T. **2006**. The Igraph Software Package for Complex Network Research. InterJournal. *Complex Systems*. 1695.

Daws MI, Mullins CE, Burslem DFRP, Paton SR, Dalling JW. **2002**. Topographic position affects the water regime in a semideciduous tropical forest in Panamá. *Plant and Soil* **238**: 79–89.

Deans RM, Brodribb TJ, Busch FA, Farquhar GD. **2020**. Optimization can provide the fundamental link between leaf photosynthesis, gas exchange and water relations. *Nature Plants* **6**: 1116–1125.

Díaz S, Kattge J, Cornelissen JHC, Wright IJ, Lavorel S, Dray S, Reu B, Kleyer M, Wirth C, Colin Prentice I *et al*. 2016. The global spectrum of plant form and function. *Nature* **529**: 167–171.

Drake PL, Froend RH, Franks PJ. **2013**. Smaller, faster stomata: scaling of stomatal size, rate of response, and stomatal conductance. *Journal of Experimental Botany* **64**: 495–505.

Drucker DP, Costa FRC, Magnusson WE. **2008**. How wide is the riparian zone of small streams in tropical forests? A test with terrestrial herbs. *Journal of Tropical Ecology* **24**: 65–74.

Emilio T, Pereira H Jr, Costa FRC. **2021**. Intraspecific variation on palm leaf traits of co-occurring species — does local hydrology play a role? *Frontiers in Forests and Global Change* **4**.

Esteban EJL, Castilho CV, Melgaço KL, Costa FRC. **2021**. The other side of droughts: wet extremes and topography as buffers of negative drought effects in an Amazonian forest. *New Phytologist* **229**: 1995–2006.

Fajardo A, Martínez‐Pérez C, Cervantes‐Alcayde MA, Olson ME. **2020**. Stem length, not climate, controls vessel diameter in two tree species across a sharp precipitation gradient. *New Phytologist* **225**: 2347–2355.

Fernández‐de‐Uña L, Martínez‐Vilalta J, Poyatos R, Mencuccini M, McDowell NG. **2023**. The role of height‐driven constraints and compensations on tree vulnerability to drought. *New Phytologist* **239**: 2083–2098.

Flores‐Moreno H, Fazayeli F, Banerjee A, Datta A, Kattge J, Butler EE, Atkin OK, Wythers K, Chen M, Anand M *et al*. 2019. Robustness of trait connections across environmental gradients and growth forms. *Global Ecology and Biogeography* **28**: 1806–1826.

Fontes CG, Fine PVA, Wittmann F, Bittencourt PRL, Piedade MTF, Higuchi N, Chambers JQ, Dawson TE. **2020**. Convergent evolution of tree hydraulic traits in Amazonian habitats: implications for community assemblage and vulnerability to drought. *New Phytologist* **228**: 106–120.

Garcia MN, Hu J, Domingues TF, Groenendijk P, Oliveira RS, Costa FRC. **2021**. Local hydrological gradients structure high intraspecific variability in plant hydraulic traits in two dominant central Amazonian tree species. *Journal of Experimental Botany* **73**: 939–952.

Gleason SM, Westoby M, Jansen S, Choat B, Hacke UG, Pratt RB, Bhaskar R, Brodribb TJ, Bucci SJ, Cao K *et al*. 2016. Weak trade-off between xylem safety and xylem‐specific hydraulic efficiency across the world 's woody plant species. *New Phytologist* **209**: 123–136.

Goldstein G, Andrade JL, Meinzer FC, Holbrook NM, Cavelier J, Jackson P, Celis A. **1998**. Stem water storage and diurnal patterns of water use in tropical forest canopy trees. *Plant, Cell and Environment* **21**: 397–406.

Gora EM, Esquivel-Muelbert A. **2021**. Implications of size-dependent tree mortality for tropical forest carbon dynamics. *Nature Plants* **7**: 384–391.

Hacke UG, Sperry JS, Pockman WT, Davis SD, McCulloh KA. **2001**. Trends in wood density and structure are linked to prevention of xylem implosion by negative pressure. *Oecologia***126**: 457–461.

Hacke UG, Spicer R, Schreiber SG, Plavcová L. **2017**. An ecophysiological and developmental perspective on variation in vessel diameter. *Plant, Cell & Environment* **40**: 831–845.

Harrison XA, Donaldson L, Correa-Cano ME, Evans J, Fisher DN, Goodwin CED, Robinson BS, Hodgson DJ, Inger R. **2018**. A brief introduction to mixed effects modelling and multi-model inference in ecology. *Peer J* **6**:e4794.

He N, Li Y, Liu C, Xu L, Li M, Zhang J, He J, Tang Z, Han X, Ye Q *et al*. 2020. Plant trait networks: improved resolution of the dimensionality of adaptation. *Trends in Ecology & Evolution* **35**: 908–918.

Jin Y, Qian H. **2022**. V.PhyloMaker2: An updated and enlarged R package that can generate very large phylogenies for vascular plants. *Plant Diversity* **44**: 335–339.

Jordan GJ, Carpenter RJ, Koutoulis A, Price A, Brodribb TJ. **2015**. Environmental adaptation in stomatal size independent of the effects of genome size. *New Phytologist* **205**: 608–617.

Kleyer M, Trinogga J, Cebrián‐Piqueras MA, Trenkamp A, Fløjgaard C, Ejrnæs R, Bouma TJ, Minden V, Maier M, Mantilla‐Contreras J *et al*. 2018. Trait correlation network analysis identifies biomass allocation traits and stem specific length as hub traits in herbaceous perennial plants. *Journal of Ecology* **107**: 829–842.

Krau JE & Arduin M. **1997**. Manual básico de métodos em morfologia vegetal. Seropédica: EDUR.

Lambers H, Oliveira RS. **2020**. Plant Water Relations. **In:** *Plant Physiological Ecology*. Springer, Cham.

Liu C, Li Y, He N. **2022**. Differential adaptation of lianas and trees in wet and dry forests revealed by trait correlation networks. *Ecological Indicators* **135**: 108564.

Liu F, Yang W, Wang Z, Xu Z, Liu H, Zhang M, Liu Y, An S, Sun S. **2010**. Plant size effects on the relationships among specific leaf area, leaf nutrient content, and photosynthetic capacity in tropical woody species. *Acta Oecologica* **36**: 149–159.

Marca‐Zevallos MJ, Moulatlet GM, Sousa TR, Schietti J, Coelho L de S, Ramos JF, Lima Filho D de A, Amaral IL, de Almeida Matos FD, Rincón LM *et al*. 2022. Local hydrological conditions influence tree diversity and composition across the Amazon basin. *Ecography* **2022**.

Messier J, McGill BJ, Enquist BJ, Lechowicz MJ. **2017a**. Trait variation and integration across scales: is the leaf economic spectrum present at local scales? *Ecography* **40**: 685–697.

Messier J, Lechowicz MJ, McGill BJ, Violle C, Enquist BJ. **2017b**. Interspecific integration of trait dimensions at local scales: the plant phenotype as an integrated network. *Journal of Ecology* **105**: 1775–1790.

Messier J, Violle C, Enquist BJ, Lechowicz MJ, McGill BJ. **2018**. Similarities and differences in intrapopulation trait correlations of co‐occurring tree species: consistent water‐use relationships amid widely different correlation patterns. *American Journal of Botany* **105**: 1477–1490.

Morris H, Gillingham MAF, Plavcová L, Gleason SM, Olson ME, Coomes DA, Fichtler E, Klepsch MM, Martínez‐Cabrera HI, McGlinn DJ *et al*. **2018**. Vessel diameter is related to amount and spatial arrangement of axial parenchyma in woody angiosperms. *Plant, Cell & Environment* **41**: 245–260.

Oliveira RS, Costa FRC, van Baalen E, de Jonge A, Bittencourt PR, Almanza Y, Barros F de V, Cordoba EC, Fagundes MV, Garcia S *et al*. **2019**. Embolism resistance drives the distribution of Amazonian rainforest tree species along hydro‐topographic gradients. *New Phytologist* **221**: 1457–1465.

Oliveira RS, Eller CB, Barros F de V, Hirota M, Brum M, Bittencourt P. **2021**. Linking plant hydraulics and the fast–slow continuum to understand resilience to drought in tropical ecosystems. *New Phytologist* **230**: 904–923.

Olson ME, Anfodillo T, Rosell JA, Petit G, Crivellaro A, Isnard S, León-Gómez C, Alvarado-Cárdenas LO, Castorena M. **2014**. Universal hydraulics of the flowering plants: vessel diameter scales with stem length across angiosperm lineages, habits and climates. *Ecology Letters* **17**: 988–997.

Olson ME, Rosell JA. **2013**. Vessel diameter–stem diameter scaling across woody angiosperms and the ecological causes of xylem vessel diameter variation. *New Phytologist* **197**: 1204–1213.

Phillips NG, Ryan MG, Bond BJ, McDowell NG, Hinckley TM, Cermak J. **2003**. Reliance on stored water increases with tree size in three species in the Pacific Northwest. *Tree Physiology* **23**: 237–245.

Poorter L, Bongers F. **2006**. Leaf traits are good predictors of plant performance across 53 rain forest species. *Ecology* **87**: 1733–1743.

Poorter L, McDonald I, Alarcón A, Fichtler E, Licona J, Peña‐Claros M, Sterck F, Villegas Z, Sass‐Klaassen U. **2009**. The importance of wood traits and hydraulic conductance for the performance and life history strategies of 42 rainforest tree species. *New Phytologist* **185**: 481–492.

Poorter L, McNeil A, Hurtado V, Prins HHT, Putz FE. **2014**. Bark traits and life‐history strategies of tropical dry‐ and moist forest trees. *Functional Ecology* **28**: 232–242.

Pratt RB, Jacobsen AL. **2017**. Conflicting demands on angiosperm xylem: trade-offs among storage, transport and biomechanics. *Plant, Cell & Environment* **40**: 897–913.

Reich PB. **2014**. The world-wide 'fast-slow' plant economics spectrum: a traits manifesto. *Journal of Ecology* **102**: 275–301.

Reich PB, Wright IJ, Cavender‐Bares J, Craine JM, Oleksyn J, Westoby M, Walters MB. **2003**. The Evolution of Plant Functional Variation: Traits, Spectra, and Strategies. *International Journal of Plant Sciences* **164**: S143–S164.

Revell LJ. **2012**. phytools: An R package for phylogenetic comparative biology (and other things). *Methods in Ecology and Evolution* **3** 217-223.

Ribeiro JELS, Hopkins MJG, Vicentini A, Sothers CA, Costa MAS, Brito JM, Souza MAD, Martins LHP, Lohmann LG, Assunção PACL *et al*. **1999**. *Flora da reserva Ducke: guia de identificação das plantas vasculares de uma floresta de terra-firme na Amazônia Central*. Manaus, Brasil: INPA.

Rosas T, Mencuccini M, Barba J, Cochard H, Saura‐Mas S, Martínez‐Vilalta J. **2019**. Adjustments and coordination of hydraulic, leaf and stem traits along a water availability gradient. *New Phytologist* **223**: 632–646.

Rosell JA, Olson ME, Anfodillo T. **2017**. Scaling of Xylem Vessel Diameter with Plant Size:

Causes, Predictions, and Outstanding Questions. *Current Forestry Reports* **3**: 46–59.

Ryan MG, Phillips N, Bond BJ. **2006**. The hydraulic limitation hypothesis revisited. *Plant, Cell and Environment* **29**: 367–381.

Ryan MG, Yoder BJ. **1997**. Hydraulic limits to tree height and tree growth. *BioScience* **47**: 235–242.

Santiago LS, De Guzman ME, Baraloto C, Vogenberg JE, Brodie M, Hérault B, Fortunel C, Bonal D. **2018**. Coordination and trade‐offs among hydraulic safety, efficiency and drought avoidance traits in Amazonian rainforest canopy tree species. *New Phytologist* **218**: 1015–1024.

Schietti J, Emilio T, Rennó CD, Drucker DP, Costa FRC, Nogueira A, Baccaro FB, Figueiredo F, Castilho CV, Kinupp V *et al*. **2014**. Vertical distance from drainage drives floristic composition changes in an Amazonian rainforest. *Plant Ecology & Diversity* **7**: 241–253.

Simioni PF, Emílio T, Giles AL, Viana de Freitas G, Silva Oliveira R, Setime L, Pierre Vitoria A, Pireda S, Vieira da Silva I, Da Cunha M. **2023**. Anatomical traits related to leaf and branch hydraulic functioning on Amazonian savanna plants. *AoB PLANTS* **15**.

Smith SA, Brown JW. **2018**. Constructing a broadly inclusive seed plant phylogeny. *American Journal of Botany* **105**: 302–314.

Sousa TR, Schietti J, Ribeiro IO, Emílio T, Fernández RH, ter Steege H, Castilho CV, Esquivel‐Muelbert A, Baker T, Pontes‐Lopes A *et al*. **2022**. Water table depth modulates productivity and biomass across Amazonian forests. *Global Ecology and Biogeography* **31**: 1571–1588.

Tng DYP, Apgaua DMG, Ishida YF, Mencuccini M, Lloyd J, Laurance WF, Laurance SGW. **2018**. Rainforest trees respond to drought by modifying their hydraulic architecture. *Ecology and Evolution* **8**: 12479–12491.

Tyree MT, Ewers FW. **1991**. The hydraulic architecture of trees and other woody plants. *New Phytologist* **119**: 345–360.

Westoby M, Falster DS, Moles AT, Vesk PA, Wright IJ. **2002**. Plant ecological strategies: some leading dimensions of variation between species. *Annual Review of Ecology and Systematics* **33**: 125–159.

Wright IJ, Reich PB, Westoby M, Ackerly DD, Baruch Z, Bongers F, Cavender-Bares J, Chapin T, Cornelissen JHC, Diemer M *et al*. 2004. The worldwide leaf economics spectrum. *Nature* **428**: 821–827.

Xiong D, Flexas J. **2020**. From one side to two sides: the effects of stomatal distribution on photosynthesis. *New Phytologist* **228**: 1754–1766.

Table 1 List of the 11 functional traits related to water-use used in this study.

Abv.	Trait	Units	Function
H	tree height	m	Light-capture, competitive ability, hydraulic path length
Dh	branch hydraulically weighted mean vessel diameter	μm	Sap conduction, hydraulic efficiency/safety
VD	branch vessel density	mm^{-2}	Wood structure, sap conduction, hydraulic efficiency/safety
SL	stomatal pore length (*proxy* for stomatal size)	μm	Gas exchange, carbon acquisition, evapotranspiration
SD	stomatal density	mm^{-2}	Gas exchange, carbon acquisition, evapotranspiration
As.Ba	stem sapwood area to basal area ratio	–	Wood structure, mechanical support, hydraulic efficiency/safety
WD	stem wood density	$g\ cm^{-3}$	Wood structure, mechanical support, hydraulic efficiency/safety
BD	branch bark density	$g\ cm^{-3}$	Bark structure, mechanical support, water storage
BT	branch bark thickness	cm	Bark structure, cambium protection, water storage
SLA	specific leaf area	$cm^2\ g^{-1}$	Leaf structure, carbon acquisition, evapotranspiration
Hv	branch Huber value	$cm^2\ m^{-2}$	Canopy architecture, balance between water supply and demand

Table 2 Pairs of closely-related species associated with contrasting soil-water conditions.

Family	Valley	Plateau
Burseraceae	*Protium klugii*	*Protium nitidifolium*
Burseraceae	*Protium opacum*	*Protium trifoliolatum*
Chrysobalanaceae	*Leptobalanus longistylus*	*Leptobalanus octandrus*
Chrysobalanaceae	*Licania laxiflora*	*Hymenopus heteromorphus*
Fabaceae	*Dipteryx punctata*	*Dipteryx magnifica*
Fabaceae	*Swartzia lamellata*	*Swartzia recurva*
Lecythidaceae	*Allantoma integrifolia*	*Cariniana micrantha*
Lecythidaceae	*Couratari stellata*	*Couratari guianensis*
Lecythidaceae	*Eschweilera laevicarpa*	*Eschweilera truncata*
Lecythidaceae	*Lecythis pisonis*	*Lecythis prancei*
Myristicaceae	*Virola pavonis*	*Virola venosa*
Sapotaceae	*Chrysophyllum sanguinolentum*	*Chrysophyllum ucuquirana-branca*
Sapotaceae	*Micropholis splendens*	*Micropholis williamii*
Sapotaceae	*Pouteria williamii*	*Pouteria flavilatex*

Table 3 Network structure metrics.

Network	Edge density	Average distance	Average clustering
Pooled	0.42	1.75	0.61
Valley	0.20	1.86	0.35
Plateau	0.24	1.93	0.60

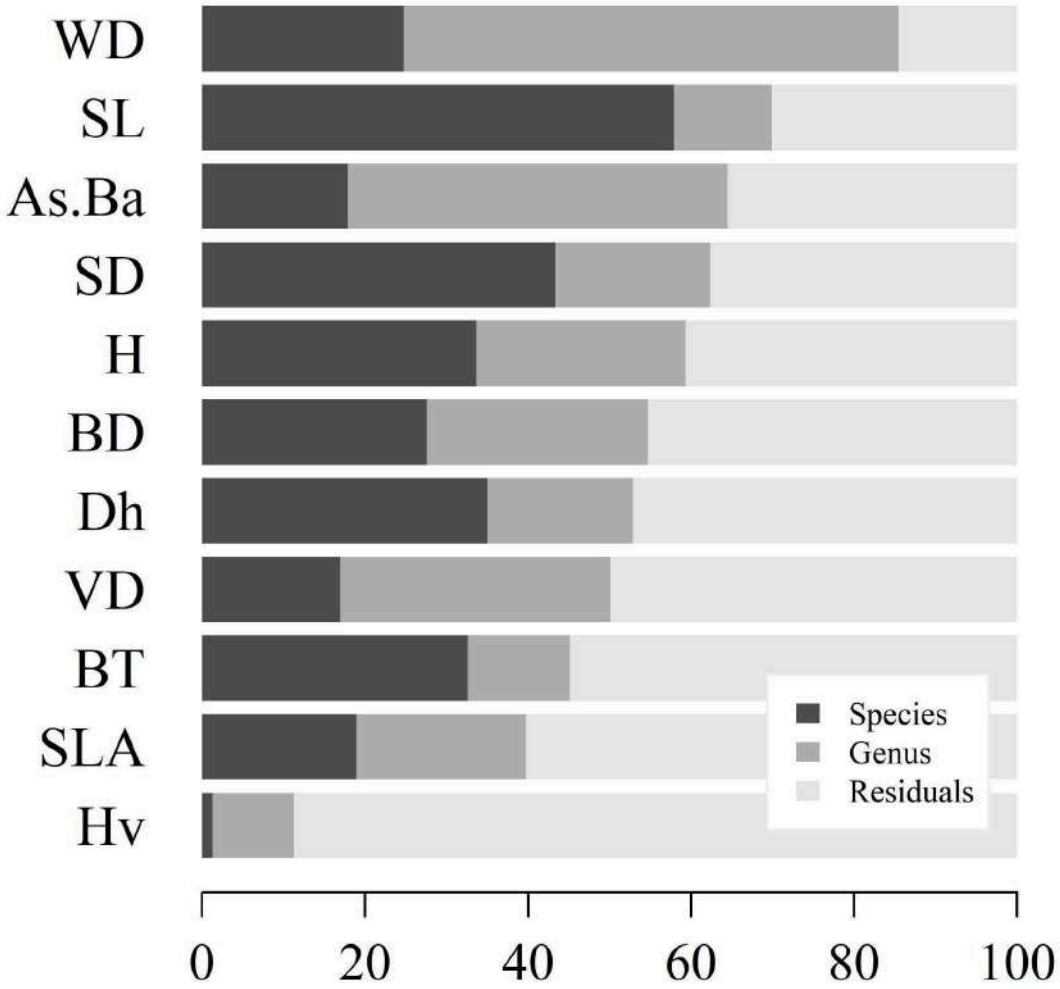

Fig. 1 Partition of variance ordered from traits with the highest proportion of variation explained by genus and species to the trait with the lowest proportion. H = tree height; Dh = branch hydraulically weighted mean vessel diameter; VD = branch vessel density; SL = stomatal pore length; SD = stomatal density; As.Ba = stem sapwood area to basal area ratio; WD = stem wood density; BD = branch bark density; BT = branch bark thickness; SLA = specific leaf area; Hv = branch Huber value.

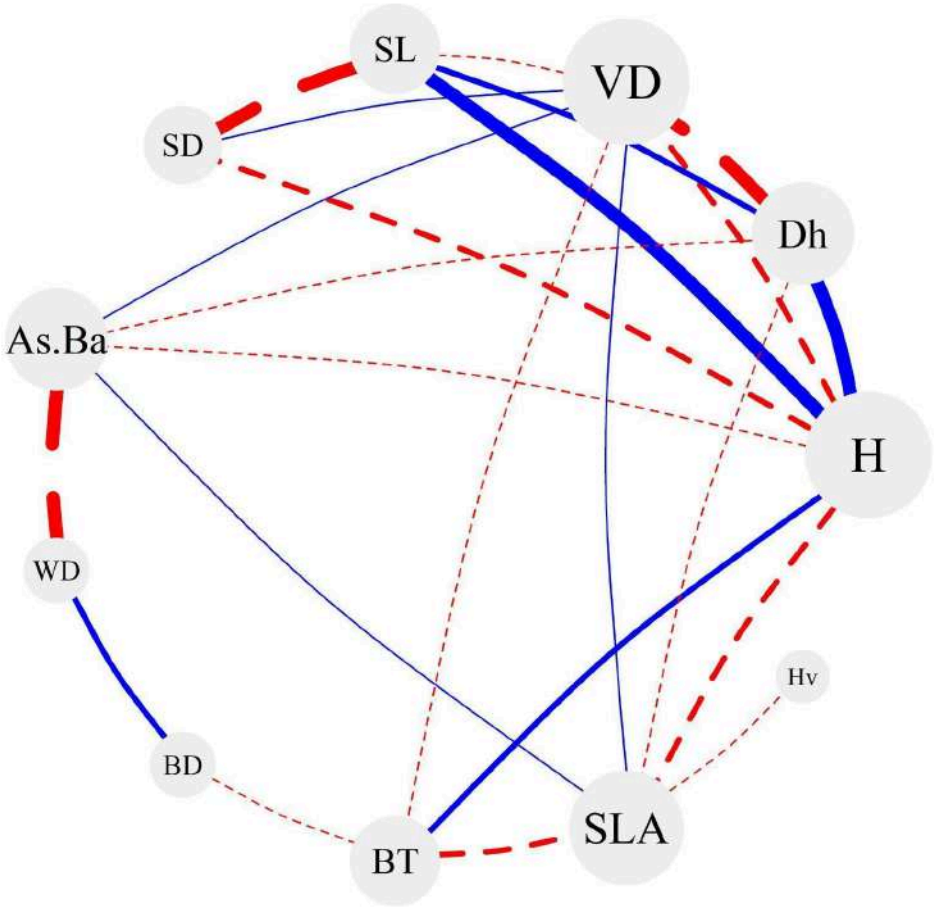

Fig. 2 Trait correlation network pooling valley and plateau species together. Blue solid lines represent positive correlations and red dashed lines negative correlations. Linewidth is weighted by Pearson's correlation coefficients: thin lines $r < 0.5$, medium-thick lines $0.5 \leq r < 0.6$, thick lines $r \geq 0.6$. Node size is weighted by trait degree. The pairwise correlations were calculated with species means (n = 28 for most traits, except for SL and SD, where n = 26). H = tree height; Dh = branch hydraulically weighted mean vessel diameter; VD = branch vessel density; SL = stomatal pore length; SD = stomatal density; As.Ba = stem sapwood area to basal area ratio; WD = stem wood density; BD = branch bark density; BT = branch bark thickness; SLA = specific leaf area; Hv = branch Huber value.

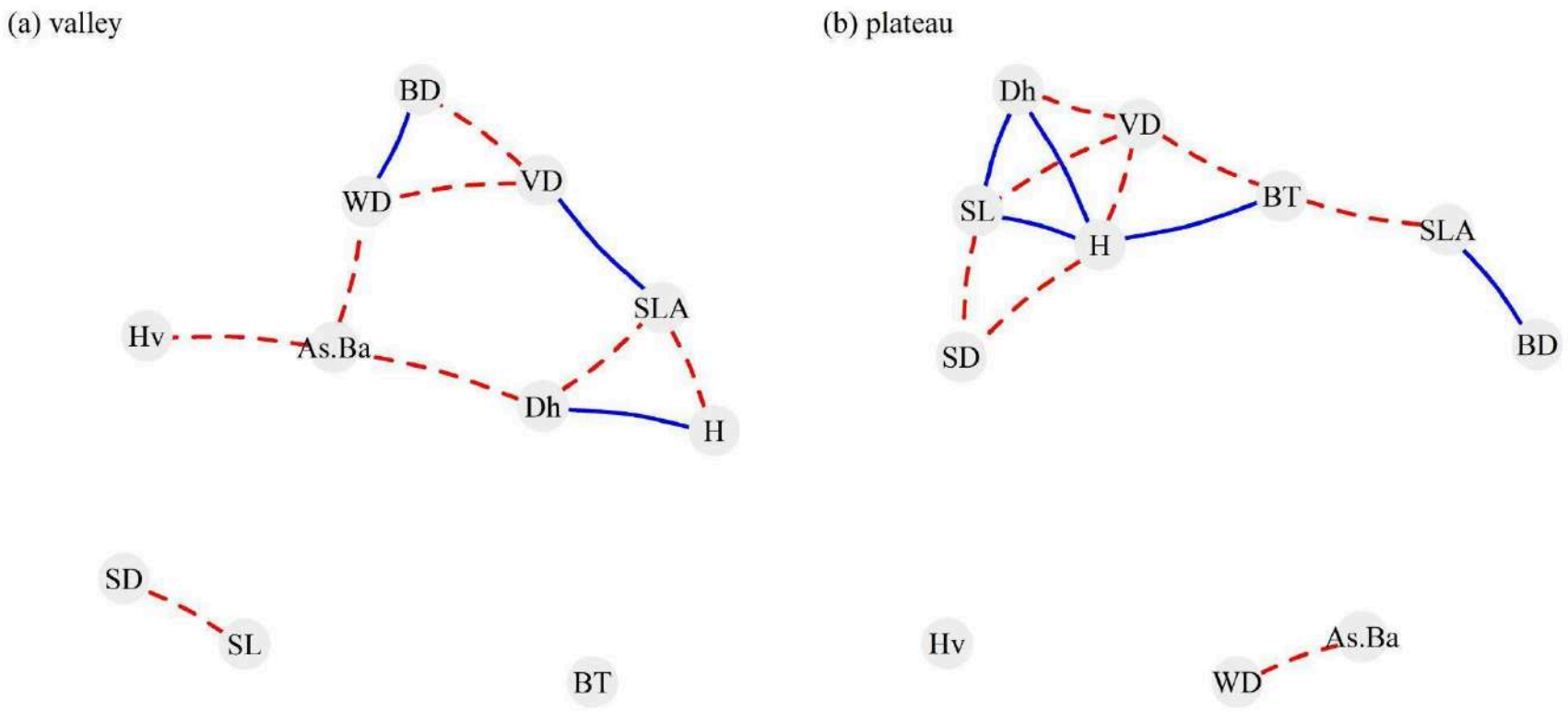

Fig. 3 Trait correlation networks of (a) valley species and (b) plateau species plotted with the Fruchterman-Reingold layout. Blue solid lines represent positive correlations and red dashed lines negative correlations. The pairwise correlations were calculated with species means (n = 14 for most traits, except for SL and SD, where n = 13). H = tree height; Dh = branch hydraulically weighted mean vessel diameter; VD = branch vessel density; SL = stomatal pore length; SD = stomatal density; As.Ba = stem sapwood area to basal area ratio; WD = stem wood density; BD = branch bark density; BT = branch bark thickness; SLA = specific leaf area; Hv = branch Huber value.

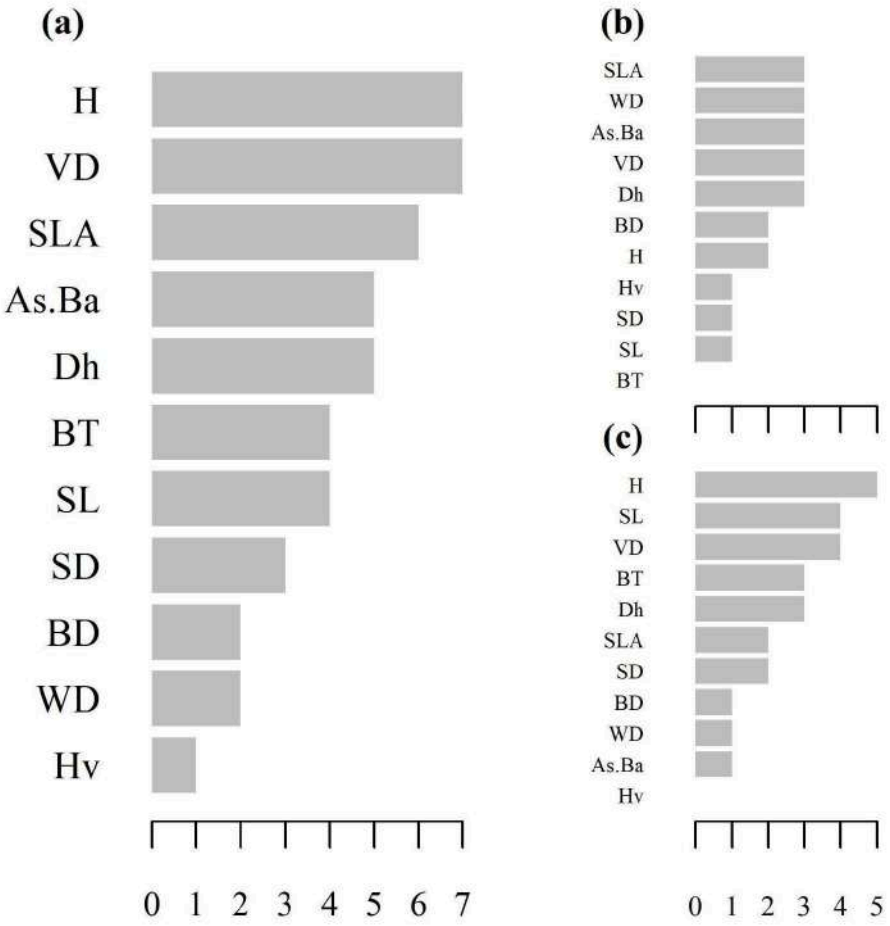

Fig. 4 Degree centralities of the 11 functional traits in the (a) pooled, (b) valley and (c) plateau networks ordered from highest to lowest degree. H = tree height; Dh = branch hydraulically weighted mean vessel diameter; VD = branch vessel density; SL = stomatal pore length; SD = stomatal density; As.Ba = stem sapwood area to basal area ratio; WD = stem wood density; BD = branch bark density; BT = branch bark thickness; SLA = specific leaf area; Hv = branch Huber value.

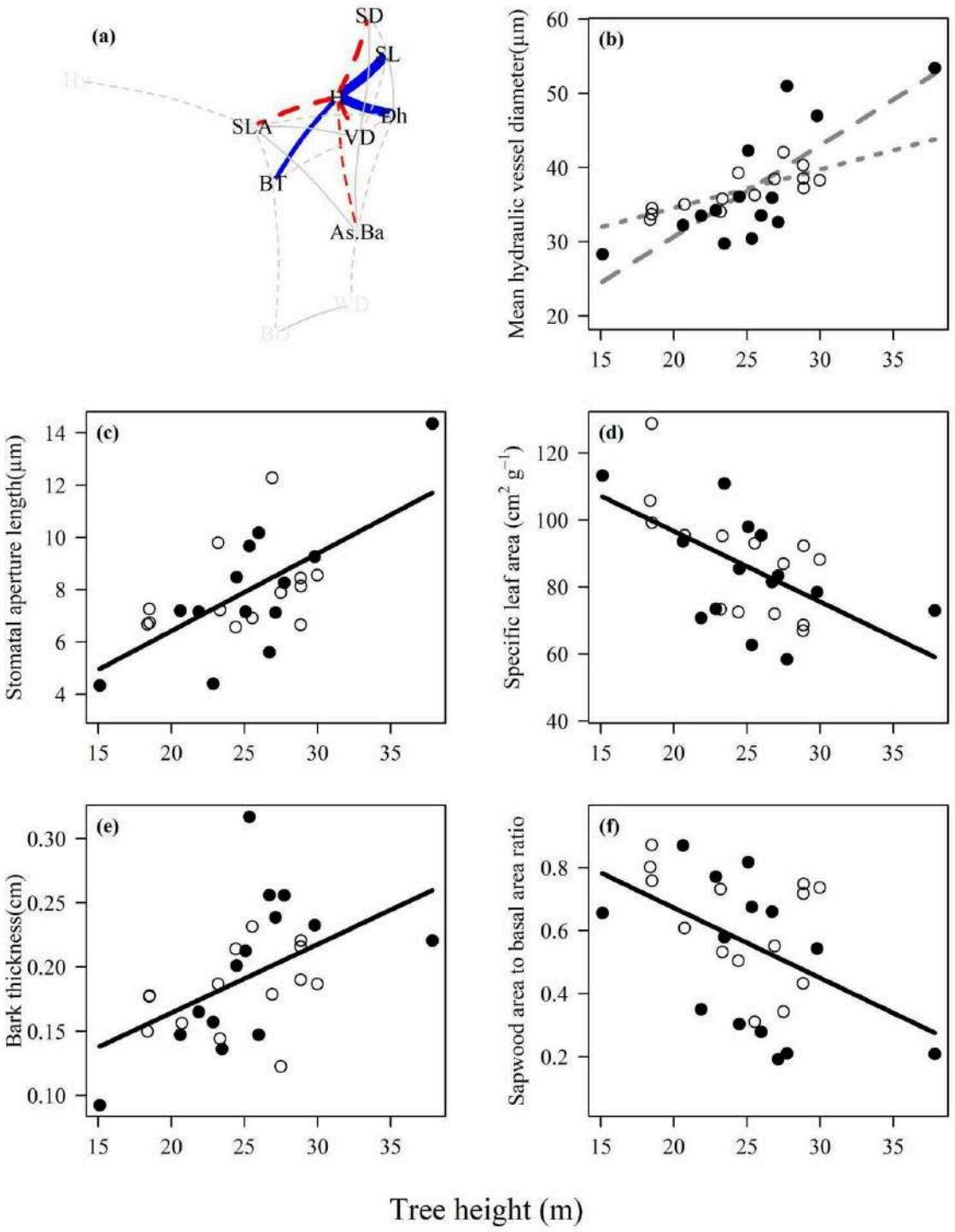

Fig. 5 Relationships with tree height linking vessel and stomatal anatomy to bark, leaf, and stem structure. The pooled network is shown in (a) with a Fruchterman-Reingold layout highlighting the links with tree height. The pair H-VD and H-SD are omitted. The solid line shows the general trend for the pooled data, while the gray dashed line represents the plateau trend and the gray dotted line the valley trend when an interaction is observed.

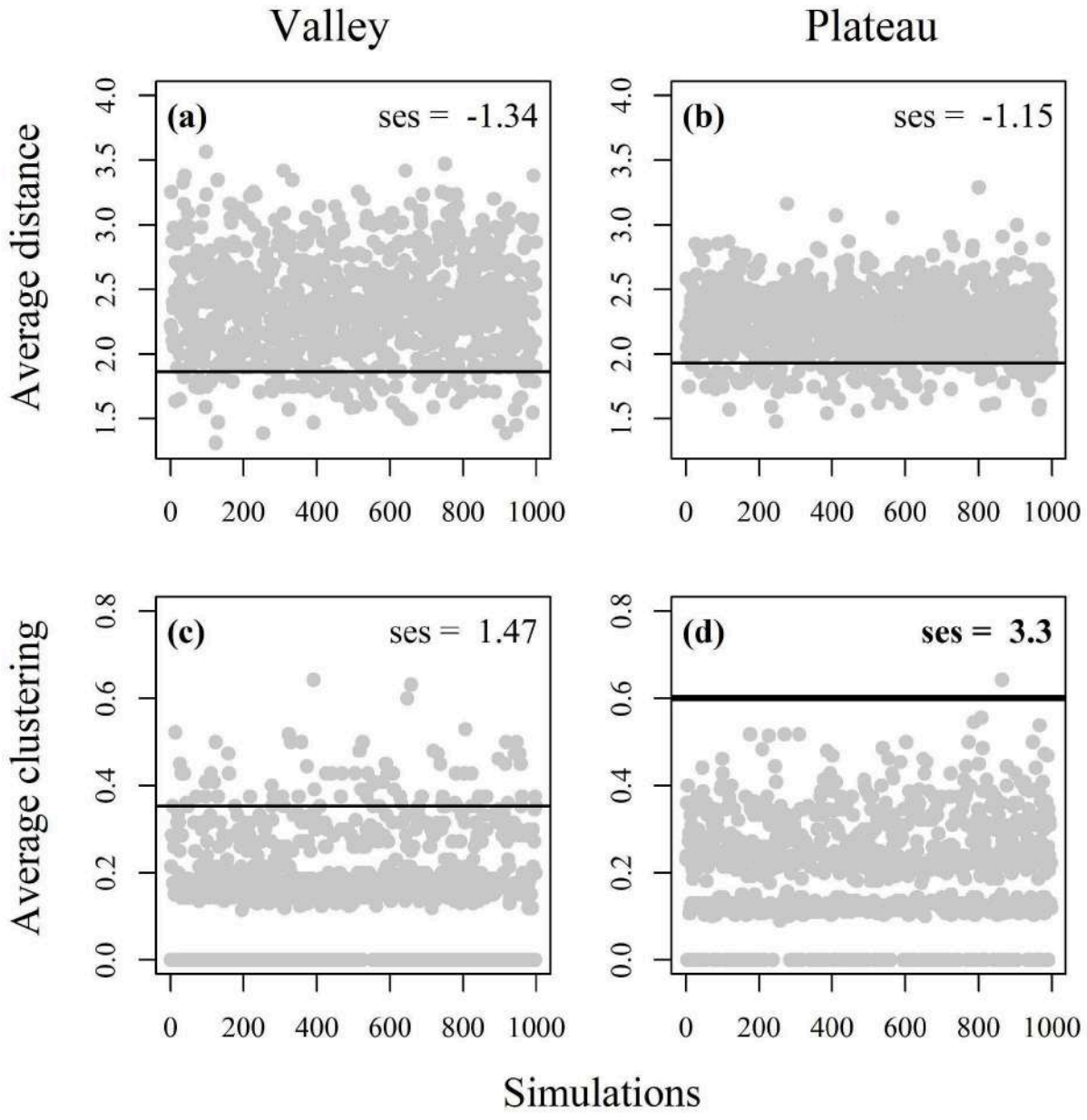

Fig. 6 Simulations of random networks and measures of average distance (a,b) and average clustering (c,d) for valley (a,c) and plateau (b,d) networks. The observed values are plotted as horizontal lines and random values as gray dots in the background. The standardized effect size (ses) comparing observed and random values is given in standard deviation units.

CONCLUSÃO GERAL

A altura das árvores é uma característica altamente integradora na arquitetura hidráulica das árvores do dossel em uma floresta da Amazônia Central. Mostramos que espécies mais altas no dossel tinham vasos e estômatos maiores e em baixa densidade, casca mais grossa, folhas com baixa área específica foliar e troncos com baixas proporções de área de alburno. Tais relações apoiam a teoria de que restrições relacionadas com a altura acoplam as economias da água e do carbono, resultando num fenótipo integrado (RYAN et al. 2006; REICH, 2014; FERNÁNDEZ-DE-UÑA et al. 2023).

Mostramos também que topologia da rede de correlação das características funcionais pode variar significativamente sob diferentes condições hidrológicas. Em particular, o agrupamento médio da rede com espécies de platô foi maior do que o esperado ao acaso, enquanto a rede com espécies de baixio tinha uma topologia mais dispersa cujo agrupamento não diferiu do acaso. A altura da árvore, a anatomia dos vasos e dos estômatos e a espessura da casca estavam intimamente ligadas entre si na arquitetura hidráulica das espécies de platô, mas não das espécies de baixio. Esses resultados sugerem uma forte integração em função do uso da água entre as espécies do platô, apoiando que as restrições relacionadas com a altura devem ser mais fortes em condições mais secas (FERNÁNDEZ-DE-UÑA et al. 2023). Espera-se, portanto, que um aumento dos regimes de seca devem impor restrições mais fortes sobre o fenótipo das espécies de platô do que sobre as espécies de baixio. No entanto, são necessários estudos que avaliem os padrões intra-específicos de variação e integração fenotípica para esclarecer como populações específicas podem responder às suas condições ambientais, ajudando-nos também a prever como o fenótipo da planta poderá responder às mudanças climáticas.

ANEXOS

New Phytologist Supporting Information

Article title: **Height-related hydraulic constraints drive a tighter integration of the hydraulic architecture of canopy trees in Central Amazon**

Authors: *Matheus G B Rosa, Luiza H M Cosme, Mirza L Bezerra, Juliana Schietti*

The following Supporting Information is available for this article:

Table S1 Species intercepts (species means) for the 11 functional traits here studied**.**

Table S2 Phylogenetic signal Pagel's lambda for each trait.

Table S3 Shortest path length (distance) between pairs of traits for the valley (below the diagonal) and plateau (above the diagonal) networks.

Table S4 Local clustering coefficient for each trait.

Notes S1 Removing extreme values in trait distribution.

Fig. S1 Pairwise relationships pooling valley and plateau species.

Fig. S2 Pairwise relationships of valley (in blue) and plateau (in orange) species considered separately.

Fig. S3 Interaction with species habitat where one habitat showed a relationship but not the other.

Fig. S4 Consistent trade-offs within the (a) branch xylem, (b) leaf epidermis, and (c) trunk wood.

Fig. S5 Updated phylogeny.

Fig. S6 The phylogenetic trait correlation network and trait degree distribution, pooling valley and plateau species with (a) $\lambda = 0$, (b) λ = mean lambda, (c) λ = maximum lambda, (d) $\lambda = 1$**.**

Table S1 Species intercepts (species means) for the 11 functional traits here studied.

Species	HAB	H	Dh	VD	SL	SD	As.Ba	WD	BD	BT	SLA	Hv
Allantoma integrifolia	vall	28.84	38.56	2.97	6.66	445.63	0.72	0.69	0.44	0.22	68.64	2.14
Cariniana micrantha	plat	37.85	53.41	1.82	14.36	187.98	0.21	0.61	0.43	0.22	73.03	1.66
Chrysophyllum sanguinolentum	vall	23.19	34.09	2.01	9.80	342.86	0.73	0.67	0.46	0.19	73.38	1.76
Chrysophyllum ucuquirana-branca	plat	25.33	30.45	2.93	9.67	316.55	0.68	0.74	0.46	0.32	62.68	1.97
Couratari stellata	vall	29.97	38.29	2.60	8.56	280.09	0.74	0.73	0.47	0.19	88.21	1.69
Couratari guianensis	plat	25.08	42.31	1.77	7.15	396.80	0.82	0.55	0.44	0.21	98.01	1.76
Dipteryx punctata	vall	27.48	42.09	2.53	7.89	417.52	0.34	0.90	0.49	0.12	86.99	1.87
Dipteryx magnifica	plat	25.96	33.55	3.06	10.18	197.39	0.28	0.95	0.60	0.15	95.40	1.89
Eschweilera laevicarpa	vall	24.40	39.27	2.50	6.57	361.09	0.50	0.83	0.45	0.21	72.56	1.77
Eschweilera truncata	plat	24.47	36.08	2.18	8.48	348.44	0.30	0.84	0.50	0.20	85.51	1.70
Lecythis pisonis	vall	25.52	36.32	2.67	6.92	335.09	0.31	0.84	0.41	0.23	93.08	2.22
Lecythis prancei	plat	27.13	32.66	2.13	7.13	379.81	0.19	0.87	0.49	0.24	83.40	1.76
Leptobalanus longistylus	vall	20.72	35.05	1.90	NA	NA	0.61	0.84	0.66	0.16	95.50	1.81
Hymenopus heteromorphus	plat	29.79	46.97	1.66	9.26	311.76	0.54	0.81	0.53	0.23	78.53	1.65
Licania laxiflora	vall	18.50	34.51	1.91	6.74	405.11	0.76	0.92	0.63	0.18	99.21	1.74
Leptobalanus octandrus	plat	23.45	29.77	3.99	NA	NA	0.58	0.79	0.63	0.14	110.91	1.80
Micropholis splendens	vall	26.89	38.48	2.83	12.28	241.22	0.55	0.68	0.58	0.18	71.98	1.98
Micropholis williamii	plat	21.86	33.50	3.92	7.15	310.42	0.35	0.80	0.43	0.17	70.77	1.83
Pouteria williamii	vall	28.83	40.33	2.67	8.45	313.57	0.43	0.76	0.42	0.19	66.99	2.38
Pouteria flavilatex	plat	27.73	51.00	1.67	8.27	487.56	0.21	0.81	0.40	0.26	58.46	2.02
Protium klugii	vall	18.48	33.74	5.37	7.27	484.26	0.87	0.53	0.42	0.18	128.86	1.76
Protium nitidifolium	plat	22.86	34.24	4.16	4.40	838.06	0.77	0.66	0.48	0.16	73.52	1.73
Protium opacum	vall	18.36	32.98	3.63	6.68	392.49	0.80	0.54	0.39	0.15	105.85	1.61
Protium trifoliolatum	plat	15.11	28.32	4.32	4.33	699.17	0.66	0.72	0.57	0.09	113.36	1.59
Swartzia lamellata	vall	23.31	35.78	2.40	7.22	372.73	0.53	0.76	0.48	0.14	95.27	1.88
Swartzia recurva	plat	26.70	35.93	3.13	5.60	398.42	0.66	0.80	0.47	0.26	81.59	1.77
Virola pavonis	vall	28.86	37.24	3.16	8.14	351.39	0.75	0.48	0.42	0.22	92.34	1.79
Virola venosa	plat	20.61	32.25	3.86	7.20	369.77	0.87	0.62	0.41	0.15	93.68	1.69

Table S2 Pagel's lambda (λ) phylogenetic signal for each trait.

Trait	Pagel's λ	logLikelihood	p-value
H	**0.48827**	**-79.93**	**0.046**
Dh	0.00007	-88.84	1.000
VD	**0.45017**	**-34.33**	**0.014**
SL	0.22059	-55.92	0.342
SD	0.34720	-162.47	0.066
As.Ba	0.30379	4.44	0.224
WD	**0.77463**	**23.13**	**0.005**
BD	**0.49760**	**35.91**	**0.011**
BT	0.19218	46.59	0.213
SLA	**0.47053**	**-113.99**	**0.005**
Hv	0.18149	8.90	0.299

Table S3 Shortest path length (distance) between pairs of traits. Distances for the valley network are presented below the diagonal, and distances for the plateau network above the diagonal. Disconnected traits show Inf values which are not computed in the calculation of the network average distance.

	H	Dh	VD	SL	SD	As.Ba	WD	BD	BT	SLA	Hv
H	-	1	1	1	1	Inf	Inf	3	1	2	Inf
Dh	1	-	1	1	2	Inf	Inf	4	2	3	Inf
VD	2	2	-	1	2	Inf	Inf	3	1	2	Inf
SL	Inf	Inf	Inf	-	1	Inf	Inf	4	2	3	Inf
SD	Inf	Inf	Inf	1	-	Inf	Inf	4	2	3	Inf
As.Ba	2	1	2	Inf	Inf	-	1	Inf	Inf	Inf	Inf
WD	3	2	1	Inf	Inf	1	-	Inf	Inf	Inf	Inf
BD	3	3	1	Inf	Inf	2	1	-	2	1	Inf
BT	Inf	Inf	Inf	Inf	Inf	Inf	Inf	Inf	-	1	Inf
SLA	1	1	1	Inf	Inf	2	2	2	Inf	-	Inf
Hv	3	2	3	Inf	Inf	1	2	3	Inf	3	-

Table S4 Local clustering coefficient for each trait. Traits with only one neighbor (degree = 1) show NA values, which are not computed in the calculation of the network average clustering.

Traits	Valley	Plateau
H	1	0.50
Dh	0.33	1
VD	0.33	0.67
SL	NA	0.67
SD	NA	1
As.Ba	0	NA
WD	0.33	NA
BD	1	NA
BT	NA	0.33
SLA	0.33	0
Hv	NA	NA

Notes S1 Removing extreme values in trait distribution.

In this study, we deleted one observation of Hv_br (individual 39369 - *Pouteria flavilatex*, with Hv_br = 11.55 cm^2 m^{-2}), and three of SLA (individuals 1646 - *Leptobalanus longistylus*, SLA = 346.29 cm^2 g^{-1}; 38640 - *Licania laxiflora*, SLA = 354.24 cm^2 g^{-1}; and NA_bolivia - *Dipteryx punctata*, SLA = 631.41 cm^2 g^{-1}). These observations were extreme values in the distribution of the individual measures of these traits, which acted as outliers in most trait-trait relationships.

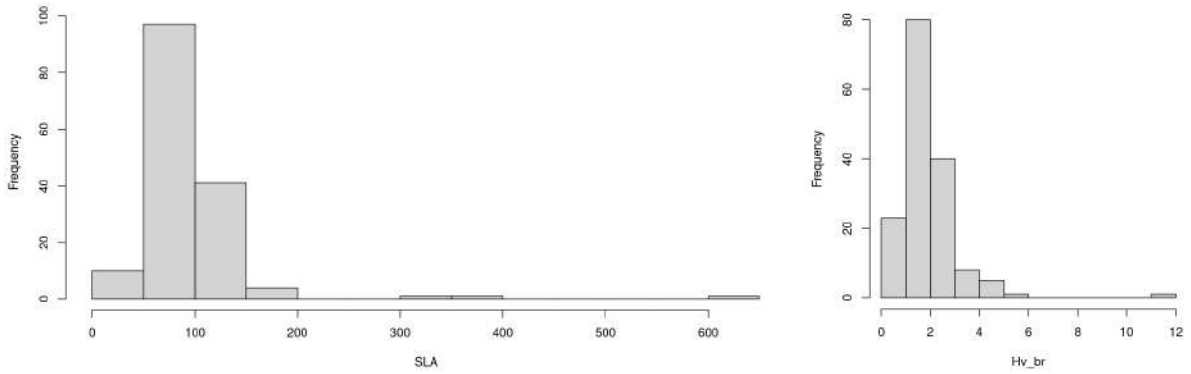

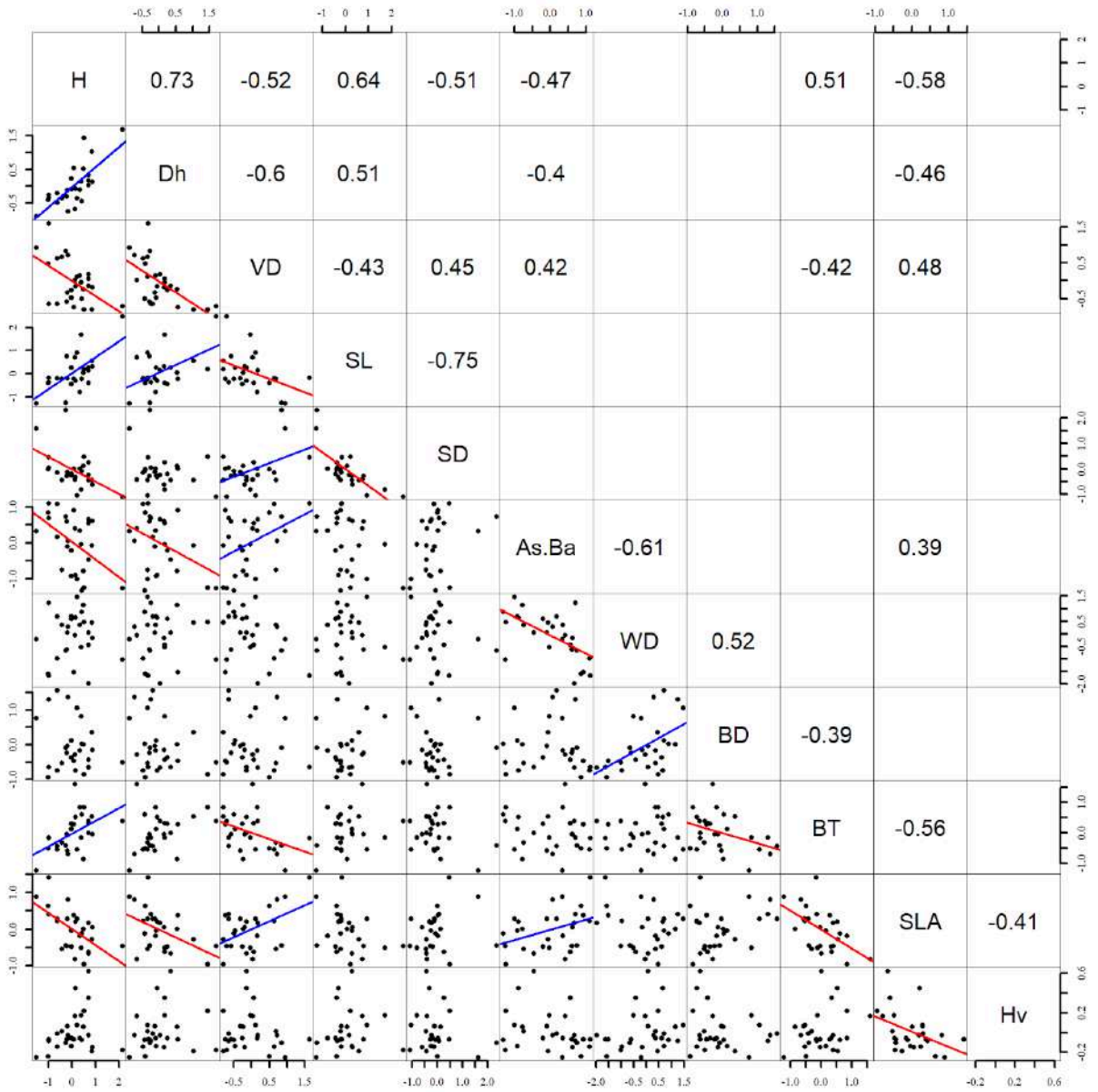

Fig. S1 Pairwise relationships between the 11 functional traits pooling valley and plateau species together. Blue solid lines represent positive correlations and red dashed lines negative correlations. Above the diagonal, only significant correlations are shown. H = tree height; Dh = branch hydraulically weighted mean vessel diameter; VD = branch vessel density; stleng = stomatal pore length; stdens = stomatal density; As.Ba = stem sapwood area to basal area ratio; WD = stem wood density; BD = branch bark density; BT = branch bark thickness; SLA = specific leaf area; Hv = branch Huber value.

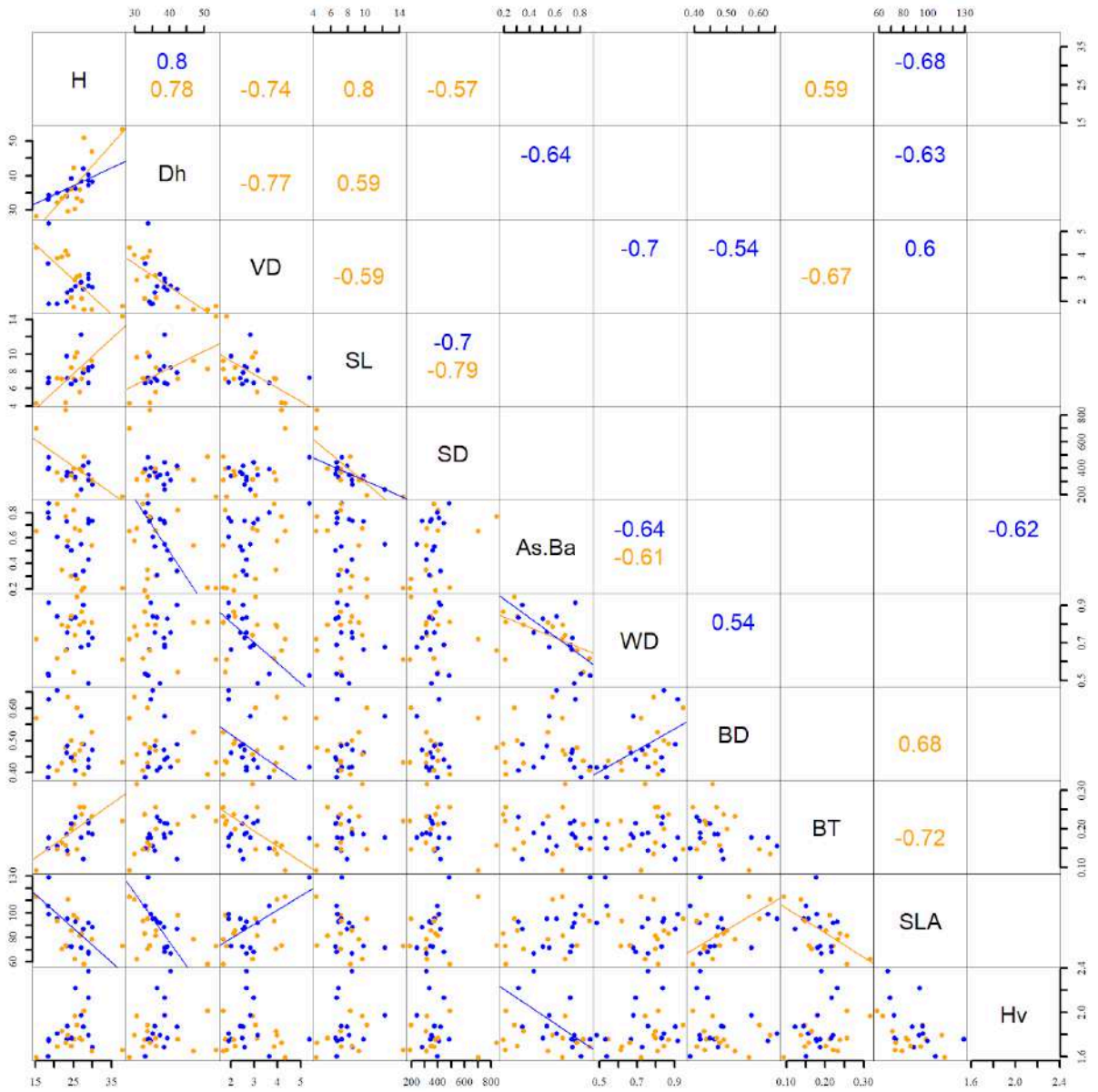

Fig. S2 Pairwise relationships between the 11 functional traits when valley (in blue) and plateau (in orange) are considered separately. Above the diagonal, only significant correlations are shown. H = tree height; Dh = branch hydraulically weighted mean vessel diameter; VD = branch vessel density; stleng = stomatal pore length; stdens = stomatal density; As.Ba = stem sapwood area to basal area ratio; WD = stem wood density; BD = branch bark density; BT = branch bark thickness; SLA = specific leaf area; Hv = branch Huber value.

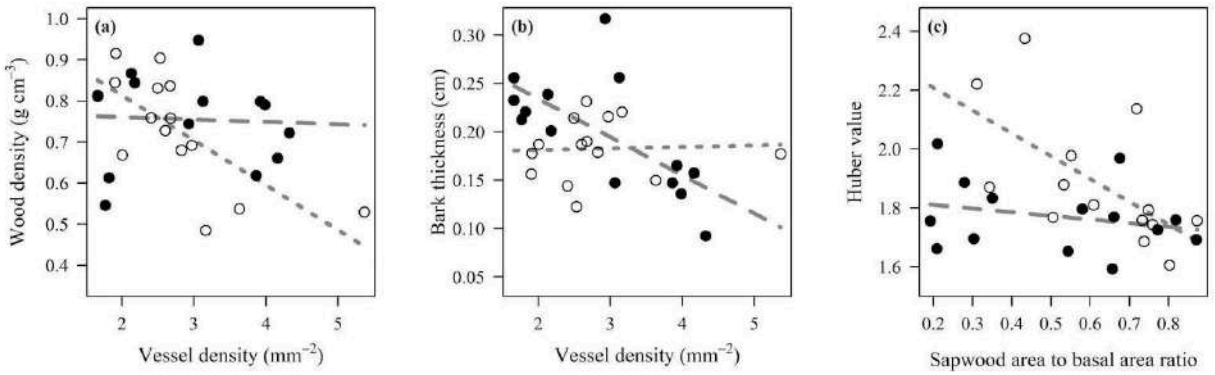

Fig. S3 Trait relationships showing significant interaction with species habitat, where one habitat showed a relationship but not the other. (a) vessel density (VD) and wood density (WD); (b) VD and bark thickness (BT); and (c) sapwood area to basal area ratio (As.Ba) and the Huber value (Hv). The dashed line represents the plateau trend and the dotted line the valley trend.

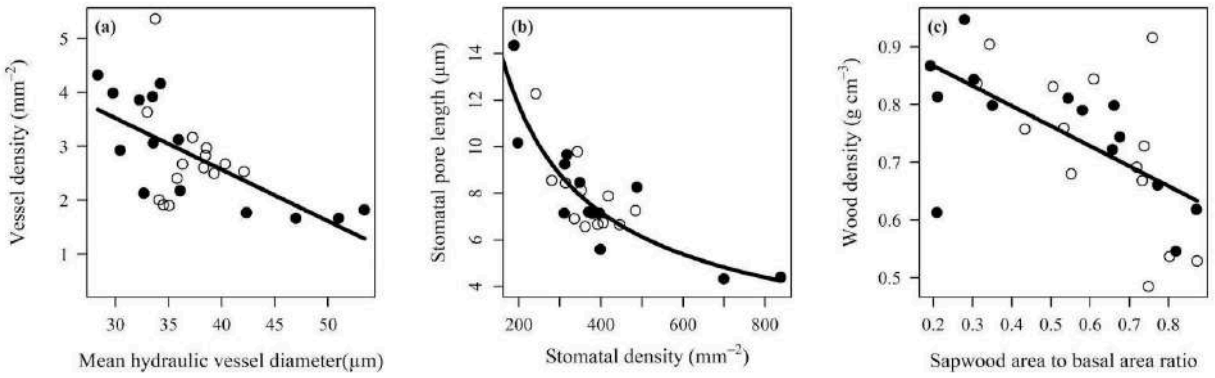

Fig. S4 Trade-offs between (a) mean hydraulic vessel diameter (Dh) and vessel density (VD); (b) stomatal density (SD) and stomatal pore length (SL); and (c) sapwood area to basal area ratio (As.Ba) and wood density (WD). Valley species are open dots and plateau species are closed dots. Only the general trend is shown because the interaction with species habitat was not significant.

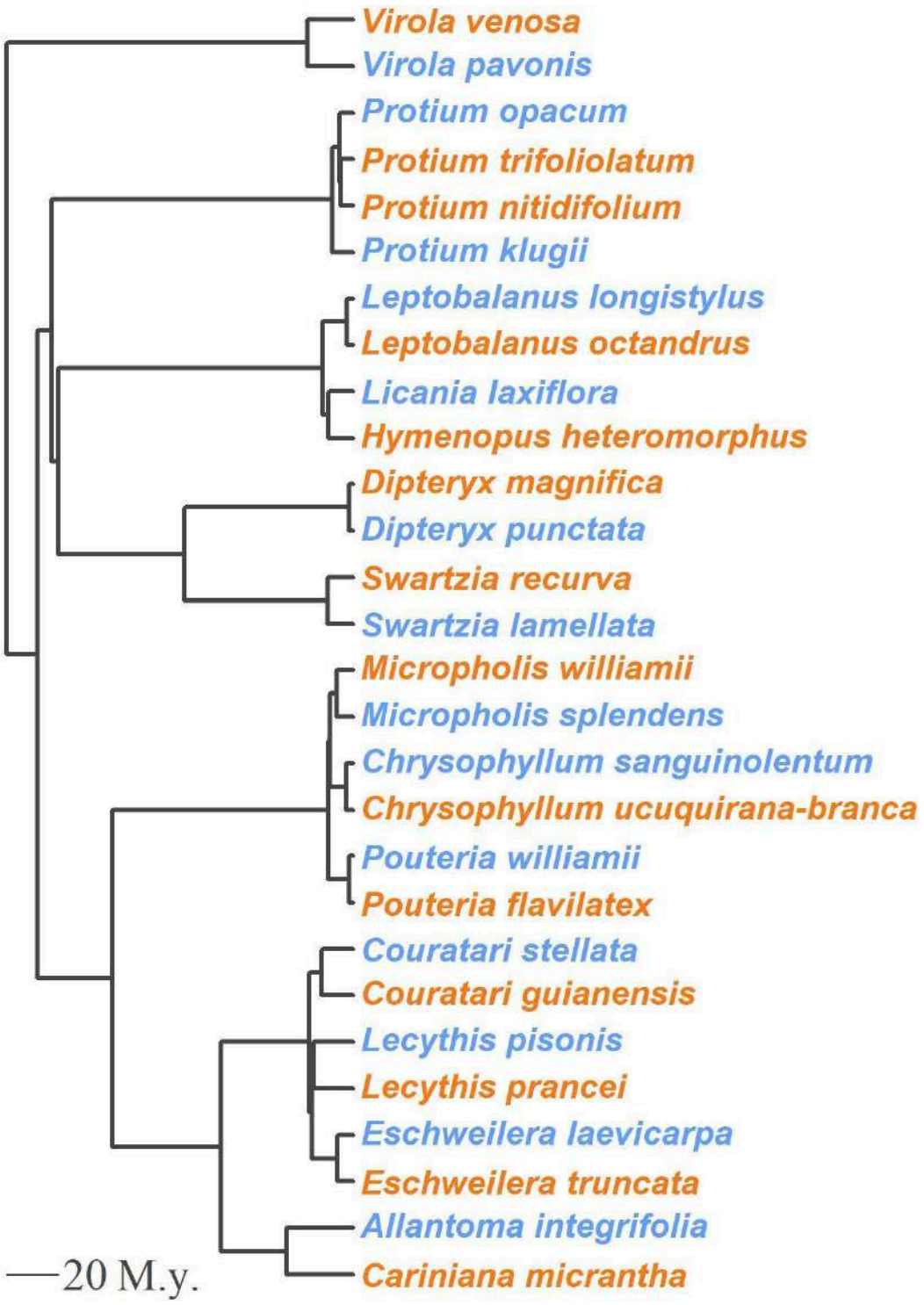

Fig. S5 Updated phylogeny pruned from the backbone GBOTB.extended.TPL (Smith & Brown 2018) in the *V.PhyloMaker2* package (Jin & Qian 2022). Species names were updated with the Flora do Brasil 2020 database.

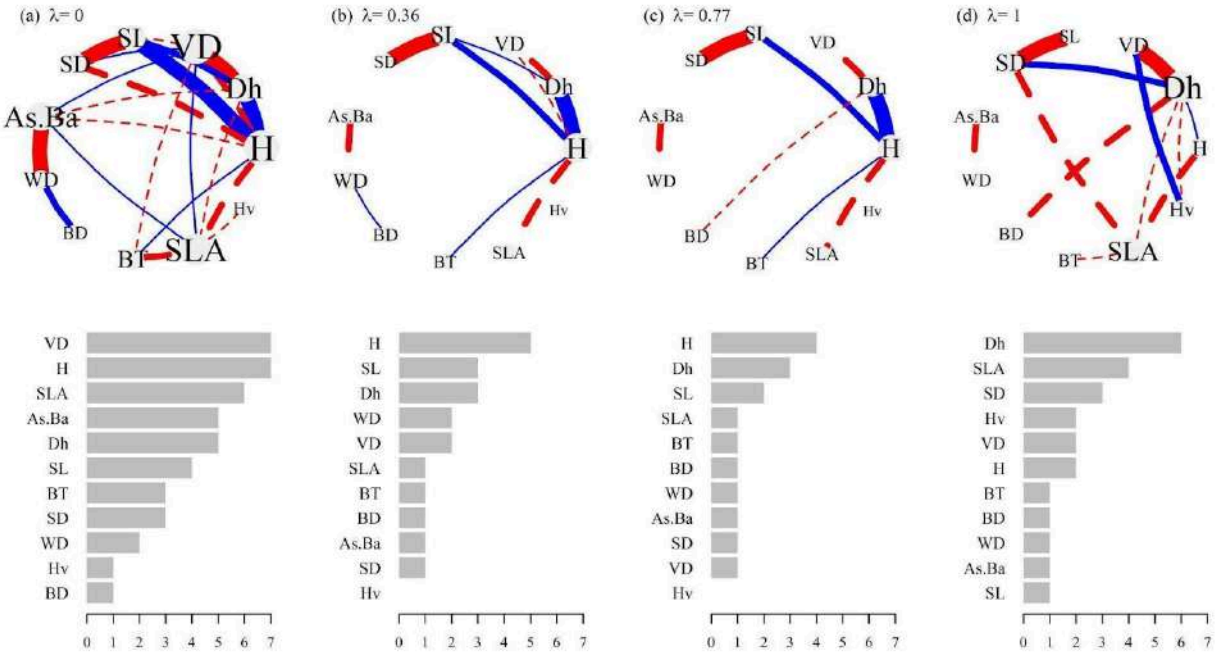

Fig. S6 The phylogenetic trait correlation network and their trait degree distribution, pooling valley and plateau species with (a) λ = 0, (b) λ = mean lambda, (c) λ = maximum lambda, (d) λ = 1. We excluded two species with missing data (*Leptobalanus octandrus* and *Leptobalanus longistylus*) to perform the phylogenetic analysis, and the pooled network excluding the same species is shown for comparison (a). Blue solid lines represent positive correlations and red dashed lines negative correlations. Linewidth is weighted by Pearson's correlation coefficients: thin lines $r < 0.5$, medium-thick lines $0.5 \leq r < 0.6$, thick lines $r \geq 0.6$. Node size is weighted by trait degree. Correlations were calculated with species means (n = 26). H = tree height; Dh = branch hydraulically weighted mean vessel diameter; VD = branch vessel density; SL = stomatal pore length; SD = stomatal density; As.Ba = stem sapwood area to basal area ratio; WD = stem wood density; BD = branch bark density; BT = branch bark thickness; SLA = specific leaf area; Hv = branch Huber value.